NUCLEIC ACID BASED IN-VITRO DIAGNOSTIC DEVICE

A THESIS SUBMITTED TO
THE GRADUATE SCHOOL OF NATURAL AND APPLIED SCIENCES
OF
MIDDLE EAST TECHNICAL UNIVERSITY

BY

OĞUZ BALCI

IN PARTIAL FULFILLMENT OF THE REQUIREMENTS
FOR
THE DEGREE OF DOCTOR OF PHILOSOPHY
IN
BIOTECHNOLOGY

JANUARY 2018

Approval of the thesis:

NUCLEIC ACID BASED IN-VITRO DIAGNOSTIC DEVICE

submitted by **OĞUZ BALCI** in partial fulfillment of the requirements for the degree of **Doctor of Philosophy in Biotechnology Department, Middle East Technical University** by,

Prof.Dr. Gülbin Dural Ünver
Dean, Graduate School of **Natural and Applied Sciences**   _____

Assoc.Prof.Dr. Can Özen
Head of Department, **Biotechnology**   _____

Assoc.Prof.Dr. Çağdaş Devrim Son
Supervisor, **Department of Biological Sciences, METU**   _____

Assoc.Prof.Dr. Can Özen
Co-Supervisor, **Department of Biotechnology, METU**   _____

Examining Committee Members:

Prof.Dr. Mesut Muyan
Department of Biological Sciences, METU   _____

Assoc.Prof.Dr. Çağdaş Devrim Son
Department of Biological Sciences, METU   _____

Assoc.Prof.Dr. Banu Balcı Peynircioğlu
Department of Medical Biology, Hacettepe University   _____

Assoc.Prof.Dr. Mecit Halil Öztop
Food Engineering Dept., METU   _____

Assoc.Prof.Dr. Didem Dayangaç Erden
Department of Medical Biology, Hacettepe University   _____

Date: 16.01.2018

I hereby declare that all information in this document has been obtained and presented in accordance with academic rules and ethical conduct. I also declare that, as required by these rules and conduct, I have fully cited and referenced all material and results that are not original to this work.

Name, Last name   : Oğuz Balcı

Signature   :

ABSTRACT

NUCLEIC ACID BASED IN-VITRO DIAGNOSTIC DEVICE

Balcı, Oğuz

Ph.D., Department of Biotechnology

Supervisor: Assoc.Prof.Dr. Çağdaş Devrim Son

Co-Supervisor: Assoc.Prof.Dr. Can Özen

January 2018, 112 pages

Commonly used nucleic acid based in-vitro diagnostic systems utilize either quantitative PCR (polymerase chain reaction) or conventional PCR. Quantitative PCR is a fast and reliable method; however, the prices of quantitative PCR devices are relatively expensive due to the cost of highly sensitive sensors. Equipment using conventional PCR is lower in price but have several disadvantages such as long analysis periods, contamination risk, false positivity risk, and usage of carcinogenic chemicals. The purpose of the study is to design, manufacture, and validate a nucleic acid based in-vitro diagnostic device operating with a novel microparticle based method. In this microparticle based method, PCR is performed with the presence of microparticles and oligonucleotide probes. Oligonucleotide probes that are unused in PCR adsorb onto the microparticles; however, fluorophore molecules released with the exo-nuclease activity of *Taq*. DNA polymerase does not adsorb onto microparticles.

By this way, background fluorescence is reduced and the need for sensitive sensors for detecting the fluorescence difference disappears.

For this purpose, a prototype device including a LED light source, two filter sliders, two excitation band-pass filters, a 24 sample carousel, two emission band-pass filters, and a CCD camera was designed and manufactured.

Microparticle batch equilibrium analysis was performed and using DNA eluates from 105 HBV negative-diagnosed and 187 HBV positive-diagnosed samples, prototype device validation study including cutoff score, analytical sensitivity, analytical specificity, linear range, precision, robustness, diagnostic sensitivity, and diagnostic specificity was conducted. The findings suggest that low-cost prototype device combines high sensitivity, specificity, reproducibility and accuracy for HBV DNA quantitation in a high linear range.

Keywords: Molecular diagnostics, HBV, quantitative PCR, microparticles, validation.

ÖZ

NÜKLEİK ASİT TABANLI VÜCÜT DIŞI TANI CİHAZI

Balcı, Oğuz

Doktora, Biyoteknoloji Bölümü

Tez Yöneticisi: Doç. Dr. Çağdaş Devrim Son

Ortak Tez Yöneticisi: Doç. Dr. Can Özen

Ocak 2018, 112 sayfa

Yaygın olarak kullanılan nükleik asit tabanlı vücut dışı tanı sistemlerinde kantitatif PZR (polymerize zincir reaksiyonu) veya konvansiyonel PZR yöntemlerini kullanılmaktadır. Kantitatif PZR hızlı ve güvenilir bir yöntemdir fakat yüksek duyarlılığa sahip sensör maliyetlerinden dolayı kantitatif PZR cihazlarının fiyatları göreceli olarak yüksektir. Konvansiyonel PZR cihazlarının maliyetleri düşüktür fakat bu yöntemde analiz sürelerinin uzun olması, kontaminasyon riskinin olması, yalancı pozitiflik riskinin olması ve kanserojenik kimyasalların kullanılması gibi dezavantajlar bulunmaktadır. Çalışmanın amacı yeni bir mikropartikül tabanlı yöntem ile çalışan, nükleik asit temelli bir vücut-dışı tanı cihazının tasarlanması, imal edilmesi ve doğrulanmasıdır. Bu mikropartikül tabanlı yöntemde, PZR, mikropartikül ve oligonükleotit probe varlığında gerçekleşmektedir. Mikropartiküller PZR esnasında kullanılmayan oligonükleotit probları üzerine almaktadır fakat *Taq.* DNA polimeraz enziminin

nükleik asitleri 5' ucundan kesme özelliğiyle açığa çıkan florofor moleküllerini üzerine almamaktadır. Böylelikle, arka plan ışıması azalmakta ve hassas sensör sistemlerine olan ihtiyaç ortadan kalkmaktadır.

Bu amaç için, bir LED ışık kaynağı, 2 eksitasyon filtresi, 24 örnek kapasiteli örnek haznesi, 2 emisyon filtresi ve bir CCD kameradan oluşan prototip cihaz tasarlanmış ve imal edilmiştir.

Mikropartikül denge analizi gerçekleştirilmiş ve prototip cihaz için eşik değeri, analitik duyarlılık, analitik özgüllük, lineer aralık, hassasiyet, sağlamlık, klinik duyarlılık ve klinik özgüllük değerlendirmelerini içeren doğrulama çalışması 105 HBV-negatif tanı konulmuş ve 187 HBV-pozitif tanı konulmuş DNA örneği kullanılarak gerçekleştirilmiştir. Bulgular düşük maliyetli prototipin, HBV DNA kantitasyonunu geniş bir lineer aralıkta yüksek duyarlılık, özgüllük, tekrarlanabilirlik ve doğrulukta gerçekleştirebildiğini göstermektedir.

Anahtar kelimeler: Moleküler tanı, HBV, kantitatif PZR, mikropartikül, doğrulama

ACKNOWLEDGEMENTS

TABLE OF CONTENTS

LIST OF TABLES

TABLES

LIST OF FIGURES

FIGURES

NOMENCLATURE

Abbreviations

$(C^0_{Pro}-C_{Pro})/C^0_{Pro}$	Solid phase (adsorbed) probe concentration per total probe concentration
C	Liquid phase solute concentration (pmol/µl)
C^0	Initial liquid phase solute concentration (pmol/µl)
$C_{particle}$	Particle concentration (µg/µl)
C^0_{Pro}	Initial liquid phase probe concentration (pmol/µl)
C_{Pro}	Liquid phase probe concentration (pmol/µl)
C_{95}	95% response concentration
CoV	Coefficient of variation
DF	Dilution Factor
dNTP	Deoxynucleotide triphosphate
DNA	Deoxyribonucleic acid
dsDNA	Double stranded deoxyribonucleic acid
ssDNA	Single stranded deoxyribonucleic acid
HBV	Hepatitis B virus
K	Linear equilibrium constant
LOD	Limit of detection
PCR	Polymerase chain reaction
RNA	Ribonucleic acid
SD	Standard deviation
q	Solid phase solute concentration (pmol solute/µg particle)
q_0	Saturation constant (pmol solute/µg particle)
T_m	Melting temperature (ºC)
y	Liquid phase solute concentration (pmol/µl)

CHAPTER 1

INTRODUCTION

This thesis focuses on development and validation of a nucleic acid based in-vitro diagnostic device operating with a novel microparticle based method.

Currently used analytical diagnostic methods are mainly based on protein and DNA analysis. Protein based methods such as electrophoresis, isoelectric focusing, SDS–PAGE, liquid chromatography, near-infrared spectroscopy, and enzyme-linked immunosorbent assay have proven to be "useful"; however, their usage is limited because of "denaturation of soluble proteins" in assays where heat treatment is applied (Violeta *et al.*, 2010). Moreover, "cross-reactions" are observed among closely related species in immunoassays where antibodies raised against a specific protein are used (Ayaz *et al.*, 2006). Violeta, *et al.* (2010) state that these problems are not experienced in nucleic acid based analytical methods since "DNA is a very stable and long-live biological molecule present in all tissues of all organisms".

"Among DNA based methods, polymerase chain reaction (PCR) is the most well developed molecular technique up to now and provides a simple, rapid, highly sensitive and specific tool" (Mafra *et al.*, 2008). Commonly used nucleic acid based in-vitro diagnostic systems utilize either quantitative PCR or conventional PCR.

Quantitative PCR is a fast and reliable method; however, the price of quantitative PCR devices is relatively expensive. High costs are mainly due to the cost of highly sensitive sensors. Equipment using conventional PCR are lower in price but have several disadvantages such as long analysis periods (4-5 hours),

contamination risk, false positivity risk, and usage of carcinogenic chemicals (ethidium bromide).

Applications of micro and nano-materials in biological reactions gathered momentum in the last decades (Priyanka *et al*., 2016). Solid-phase PCR, nano-PCR, and microparticle based DNA biosensors are the main micro and nano-material based PCR applications. Nevertheless, in the literature there is no work reporting the usage of microparticles in order to reduce background fluorescence for eliminating the need for sensitive sensors. In this study, PCR is performed with the presence of microparticles and oligonucleotide probes. Oligonucleotide probes that are unused in PCR adsorb onto the microparticles; however, fluorophore molecules released with the exo-nuclease activity of *Taq*. DNA polymerase does not adsorb onto microparticles. By this way, background fluorescence is reduced and the need for sensitive sensors for detecting the fluorescence difference disappears.

In this thesis, a nucleic acid based in-vitro diagnostic device operating with the invented microparticle based method is presented. For this purpose, a prototype nucleic acid based in-vitro diagnostic device was manufactured, microparticle batch equilibrium experiments were performed, and for quantitation of HBV DNA, prototype device validation study including cutoff score, analytical sensitivity, analytical specificity, linear range, precision, robustness, diagnostic sensitivity, and diagnostic specificity was conducted. Finally, linear equilibrium constant (K), cutoff score, limit of detection (LOD), linear range, overall statistical spread, diagnostic sensitivity, and diagnostic specificity were calculated.

2

CHAPTER 2

LITERATURE SURVEY

2.1 Diagnostic methods

"Molecular diagnostic methods have increased the ability of the clinical laboratory to detect infectious diseases and have eliminated the need for traditional culture methods in some applications" (Lynne, 2007). Morinha, *et al.* (2012) state that PCR based techniques have been evolved "overcoming some limitations of the more classical molecular analysis methodologies".

Laude, *et al.* (2016) comment that the PCR assay, compared with conventional laboratory techniques such as microscopy and ELISA, "offers attractive performances, an optimized turnaround time and is able to make a rapid identification". "DNA based detection methods display several advantages such as an increased sensitivity and specificity, and the possibility for molecular typing" (Laude *et al.*, 2016).

2.2 PCR based diagnostic methods

Morinha, *et al.* (2012) state that, following conventional PCR, agarose gel electrophoresis and/or southern hybridization were the major molecular detection tools used in research and clinical laboratories. "The quantitative PCR methodologies present great advantages over classical PCR based methods, but the traditional methods (e.g., agarose and polyacrylamide gels) continue to be important for the initial screening and evaluation of the markers" (Morinha *et al.*, 2012).

"Recently, nucleic acid amplification and detection techniques have progressed based on advances in microfluidics, microelectronics, and optical

systems. Nucleic acids amplification based point-of-care test (POCT) in resource-limited settings requires simple visual detection methods. Several biosensing methods including lateral flow immunoassays (LFIA) were previously used to visually detect nucleic acids. However, prolonged assay time, several washing steps, and a need for specific antibodies limited their use" (Hwang *et al*., 2016).

Additional confirmation methods and/or examination of PCR products can be accomplished such as sequencing of DNA amplicons (Karlsson *et al*., 2007), simultaneous amplification of two or more fragments with different primer pairs (multiplex PCR) (Tobe *et al*., 2008), digital PCR (Coren *et al*., 2014), microarrays (Teletchea *et al*., 2008), single strand conformation polymorphism (Glavac *et al*., 1993), restriction fragment length polymorphism (RFLP) (Pourzand *et al*., 1993), random amplified polymorphic DNA (RAPD) (Galvão *et al*., 2008), amplified fragment length polymorphism (Mueller *et al*., 1999), microsatellites (Guichoux *et al*., 2011), allele-specific PCR (Gaudet *et al*., 2009), capillary electrophoresis (Kleparník *et al*., 2007), and high-resolution melting analysis (Reed *et al*., 2007). "These methods are cost-effective methods but also time-consuming and moderately laborious, which limit their high-throughput applicability" (Morinha *et al*., 2012).

"Quantitative PCR (simultaneous amplification and detection of nucleic acid in a closed system), with its shortened turnaround time, flexibility for multiple applications (detection, quantification, mutation screening), and enhanced sensitivity and specificity, has led to a wider acceptance of PCR in the clinical laboratory setting" (Lynne, 2007).

2.2.1 Quantitative PCR

In quantitative PCR (United States Patent 6,814,934) the target region on the nucleic acid to be analysed is amplified with PCR (United States Patent 4,683,202). In PCR, isolated nucleic acid is mixed with PCR reagents and incubated at planned temperatures for intended time intervals. Extensively used PCR reagents are primers, *Taq.* DNA polymerase, dNTP's, PCR buffer, and

MgCl$_2$. Primers are oligonucleotides that determine the boundaries of the region to be amplified. *Taq.* DNA polymerase (United States Patent 4,889,818) performs elongation of primers using nucleic acid constituent dNTP's. PCR buffer, and MgCl$_2$ provide a basis for *Taq.* DNA polymerase to function properly. Isolated nucleic acid mixed with PCR reagents are incubated at 95°C for an intended period of time in order to denaturate double stranded DNA. Primer annealing happens with incubation at a planned temperature between 55-65°C for an intended period of time. Extension is performed by *Taq.* DNA polymerase at its optimum functioning temperature (72°C). In quantitative PCR along with the PCR reagents, oligonucleotide probes (United States Patent 5,210,015) specific to the amplified target region are used. Oligonucleotide probes are labeled with fluorophores that are excited with a light source at a specific wavelength and emits light at a higher wavelength, and a quencher that absorp the emission of the fluorophore. *Taq.* DNA polymerase degrades oligonucletide probe with its exo-nuclease activity and by this way fluorophore escapes from quenching and a slight increase in emission is observed. This slight increase is detected with highly sensitive sensors.

2.2.2 Conventional PCR

In agarose gel electrophoresis method, agarose gel is prepared and placed into electrophoresis tank filled with electric conducting buffer. PCR products are placed into the wells on the agarose gel. PCR products migrate to anode. Small molecules migrate faster than big molecules so, PCR product is analysed via molecular weight markers.

Commonly used nucleic acid based in-vitro diagnostic systems utilize either quantitative PCR or conventional PCR.

Quantitative PCR is a fast and reliable method; however, the price of quantitative PCR devices are relatively expensive; the prices range between 25,000 € and 100,000 €. High costs are mainly due to the cost of highly sensitive sensors. Equipment using the conventional PCR are lower in price (about 25,000

5

€) but have several disadvantages such as long analysis periods (4-5 hours), contamination risk, false positivity risk, and usage of carcinogenic chemicals (ethidium bromide).

2.3 Micro and nano-material based PCR assays

With the advent of nanotechnology, the use of micro and nano-materials in biological reactions has gained momentum due to the desired properties of these materials (Priyanka *et al*., 2016). Solid-phase PCR, nano-PCR, and microparticle based DNA biosensors are the main micro and nano-material based PCR applications.

In solid-phase PCR, PCR amplification is performed directly on polymer particles (Seungwon *et al*., 2017). Hua *et al*. (2011) demonstrated fluorescence quenching method for DNA detection by using gold nanoparticles functionalized with thiol-modified primers and quantum dots functionalized with amino-modified primers. Hongna *et al*. (2007) presented a methodology with PCR directly on magnetic nanoparticles and hybridization with probes labeled with dual-color fluorophores. For this purpose, biotin labelled primers were immobilized onto streptavidin labelled microparticles. After PCR, in order to gain ssDNA, washing, resuspending and denaturing steps are applied. After hybridization with probes, washing, denaturation, printing onto glass slide, scanning, image analysis were performed. Steps involved in post-PCR assays such as dsDNA denaturation, washing, ssDNA separation, immobilization, probe hybridization, enzymatic labelling, and printing increase the experimental cost and complexity in practical applications (Hongyan *et al*. 2014).

In nano-PCR, nano-materials are used in order to enhance the PCR yield with their physiochemical properties such as high thermal conductivity and surface to volume ratio (Priyanka *et al*., 2016). Carbon nanotubes (Zhang *et al*., 2008), silver nanoparticles (Wan *et al*., 2009), TiO_2 nanoparticles (Abdul *et al*., 2010), quantum dots (Liang *et al*., 2010), gold nanoparticles (Huang *et al*., 2005) magnetite nanoparticles (Priyanka *et al*., 2016) were used to enhance the PCR

yield by benefiting high thermal conductivity and surface to volume ratio of these nano-materials. In nano-PCR, optimization of PCR conditions and components as well as optimization of concentration of nanoparticles are applied leading to a gaussian curve for the nanofluids indicating a concentration dependent PCR yield that goes from inhibition to enhancement of PCR reaction (Priyanka *et al*., 2016). Wanzhe *et al*. (2015) state that, nano-PCR assays reach the target temperature more quickly and disperse the heat uniformly in the solution reducing the time at non-target temperatures which leads to a decrease in non-specific amplification. On the other hand, Toshiaki *et al*. (2015) state that the interaction between *Taq* DNA polymerase and nanomaterials has a significant negative influence on PCR efficiency as a result of reduced enzyme activity due to non-specific adsorption onto nanoparticle surfaces.

In microparticle based DNA biosensors, double strand PCR product is either conjugated with microparticles or denaturated into ssDNA, hybridized with probe and then conjugated with microparticles. For gaining ssDNA, the standard procedure (Giovanni *et al*., 2017) is to denature double strand PCR amplicon at high temperature (90–95°C) followed by shock-cooling to reduce diffusion and thus re-hybridization in solution. However, re-hybridization will still compete against target hybridization to probes leading to a decrease in sensitivity. Asymmetric PCR to produce ssDNA (Wei *et al*., 2004) and in vitro transcription to produce RNA (Petersen *et al*., 2008) have been employed to increase assay sensitivity. Giovanni *et al*. (2017) present a biosensor platform starting from an initially dsDNA target where the target strand of interest is biotinylated and detected by the sensor by linking streptavidin magnetic nanoparticles to the sensor surface. Yan *et al*. (2017) use asymmetric PCR to produce biotin labelled single strand target DNA which is then hybridized with probes and incubated with streptavidin-coated particles producing electrochemiluminescence signal. Lorena *et al*. (2016) use an electromagnetic platform that couples the hybridization recognition reaction with sequence-specific DNA probes using ssDNA (denatured PCR product) in a sandwich format with haptenmolecules on

magnetic microparticles with enzymatic labelling for electrochemical detection. Sang *et al*. (2016) suggest an assay in which biotin and Cy3 labelled PCR amplicon is mixed with streptavidin-magnetic beads and introduced into the density medium. Xiaoteng *et al*. (2010) present an immobilization-free electrochemistry based biotin labelled PCR amplicon detection approach utilizing the streptavidin-coated magnetic particles and an electro-active intercalator compound. Mahsa *et al*. (2017) uses a calorimetric detection methodology to detect ssDNA (denatured PCR amplicon) with gold nanoparticle-thiol labeled probe conjugate.

There is no work in the literature reporting the usage of microparticles in order to reduce background fluorescence for eliminating the need for sensitive sensors. In this study, PCR is performed with the presence of microparticles and oligonucleotide probes. Oligonucleotide probes that are unused in PCR adsorb onto the microparticles; however, fluorophore molecules released with the exo-nuclease activity of *Taq*. DNA polymerase does not adsorb onto microparticles. By this way, background fluorescence is reduced and the need for sensitive sensors for detecting the fluorescence difference disappears.

2.3.1 Decreasing PCR background fluorescence via microparticles

In this study, microparticles are used in order to reduce background fluorescence for eliminating the need for sensitive sensors (microparticle working mechanism is given in Figure 2.1).

Oligonucleotide probes used in quantitative PCR are labelled with a fluorophore that is emitting light when excited and a quencher that absorp a part of the emission of the fluorophore. In quantitative PCR, *Taq*. DNA polymerase degrades oligonucletide probes with its exo-nuclease activity and by this way fluorophore escapes from quenching leading to an increase in emission. On the other hand, excess/unused oligonucleotide probes (oligonucleotide probes that are not degraded by *Taq*. DNA polymerase during PCR) also emits light resulting in background fluorescence emission (noise). Therefore, the fluorescence emission

8

difference between positive and negative sample turns out to be small and can only be detected with sensitive sensors.

In the developed microparticle based PCR method, oligonucleotide probes that are excess/unused in PCR adsorb onto the microparticles; however, fluorophore molecules released with the exo-nuclease activity of *Taq.* DNA polymerase does not adsorb onto microparticles. By this way, liquid-phase fluorescence emission difference between positive and negative samples increases since background fluorescence emission (noise) is reduced. As a result, the need for sensitive sensors for detecting the fluorescence difference disappears.
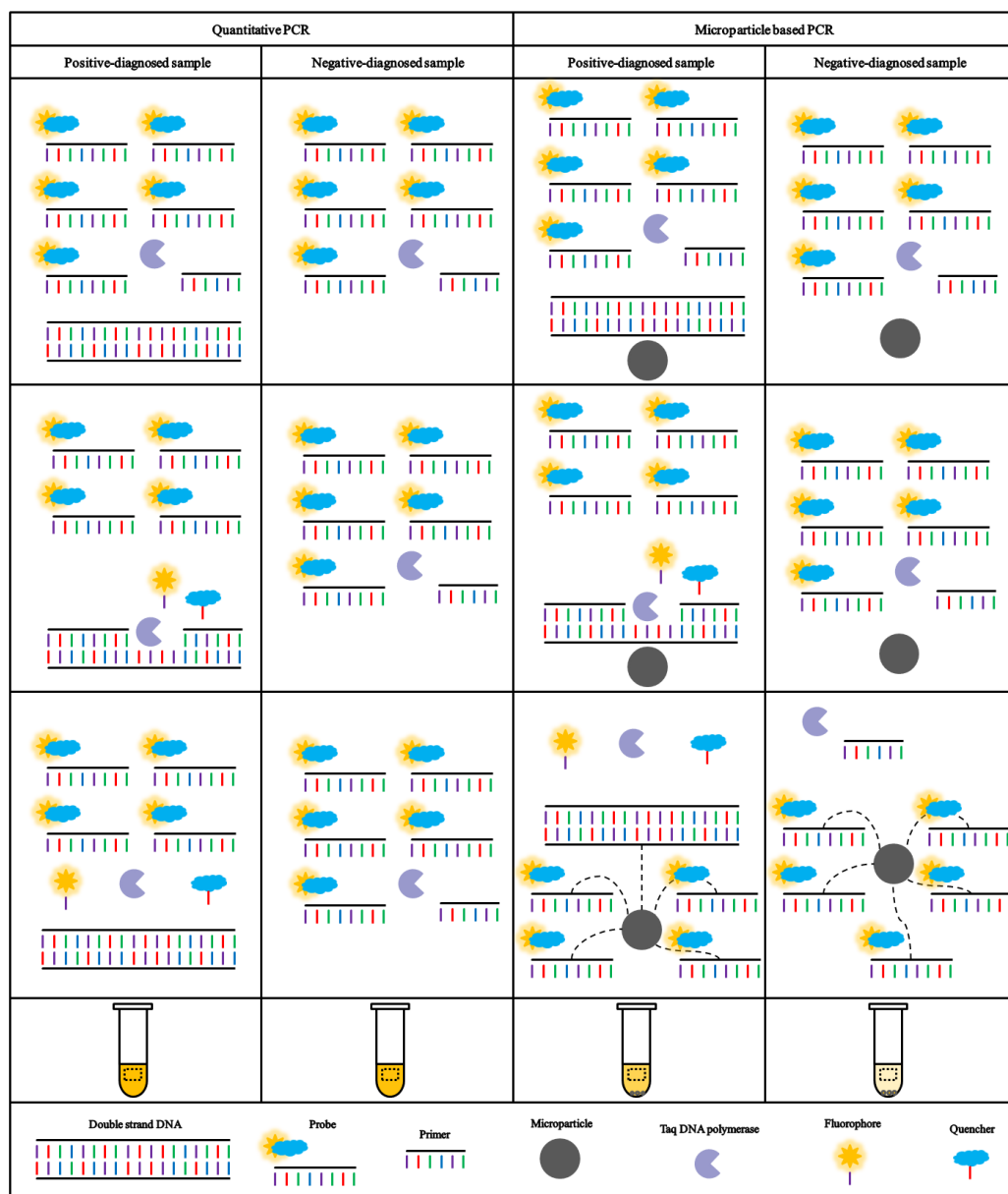
Figure 2. 1 Microparticle working mechanism

In quantitative PCR, excess/unused oligonucleotide probes (oligonucleotide probes that are not degraded by *Taq.* DNA polymerase during PCR) emit light resulting in background fluorescence emission (noise). In microparticle based PCR, oligonucleotide probes that are excess/unused in PCR adsorb onto the microparticles; however, fluorophore molecules released with the exo-nuclease activity of *Taq.* DNA polymerase does not adsorb onto microparticles.

2.3.2 Adsorption and adsorption isotherms

Two types of adsorption may occur (Smith, 1983):

a) Physical adsorption: is nonspecific and the atomic or molecular forces attracting the molecules in the fluid to the solid surface are relatively weak, and the heat evolved during the exothermic adsorption process is of the same order of magnitude as the heat of condensation ($-\Delta H = 0.5$ to 5 kcal/mol).

b) Chemical adsorption or chemisorption: is specific and involves forces much stronger than in physical adsorption. The adsorbed molecules are held to the active sites or immobilized ligands by valence forces of the same type as those occurring between atoms in molecules.

"Analysis of an adsorption process is based on identifying an equilibrium relationship between bound and free solute and performing a solute material balance. The equilibrium relationship between the solute concentration in the liquid phase and that on the adsorbent's surface at a given condition is called an isotherm" (Raja, 2006). From the point of view of bioseparations, three types of isotherms:

1. Linear adsorption,
2. Freundlich adsorption, and
3. Langmuir adsorption

are important. Most isotherms are linear when the solute concentration is very low. The linear isotherm is given by:

$$q = Ky \qquad\qquad (2.1)$$

where q is the amount of solute adsorbed per amount of adsorbent, y is the solute concentration in solution, and K is linear equilibrium constant.

The adsorption of antibiotics, steroids and hormones generally follow Freundlich type isotherm:

$$q = Ky^n \qquad\qquad (2.2)$$

where the constants n and K must be determined experimentally. These constants are best determined by means of log-log plot of q versus y.

The Langmuir isotherm is applicable when there is a strong specific interaction between the solute and the adsorbent. Ion exchange and affinity type adsorptions generally follow Langmuir isotherm:

$$q = yq_0 / (K+y) \qquad (2.3)$$

in which q_0 and K are constants which must be determined experimentally. The constants are best determined by means of a plot of q^{-1} versus y^{-1}. The intercept on such a plot is q_0^{-1} and the slope is K/q_0.

$$q^{-1} = Ky^{-1}q_0^{-1} + q_0^{-1} \qquad (2.4)$$

2.4 Diagnostics of HBV infection

"Hepatitis B virus (HBV) is a double-stranded DNA virus of the *Hepadnaviridae* family that causes both acute and chronic hepatitis" (Paraskevis *et al*., 2002). According to the World Health Organization estimates, 2 billion people have been infected with HBV worldwide and more than 350 million have persistent infection (http://www.who.org/).

"Quantitative assays of the HBV DNA are used extensively to determine the presence of infection as well as to assess the response to treatment" (Berger *et al*., 2001). In Table 2.1, published studies and commercial assays are given with limit of detection and linear range information.

Table 2. 1 Published studies and commercial assays for HBV diagnosis

Limit of detection ($\log_{10}$ concentration copy/ml)	Linear range ($\log_{10}$ concentration copy/ml)	Source
2.02	2.02 – 8.92	www.roche.com
2.05	2.05 - 11.75	www.qiagen.com
2.13	2.13 – 11.13	(Garson *et al*., 2005)
2.14	2.14 - 9.75	www.rtalabs.com.tr
2.17	2.17 – 8.17	www.abbott.com
2.39	2.39 – 10.39	(Kavita *et al*., 2006)
2.4	2.4 - 11.4	(Paraskevis *et al*., 2002)
2.53	2.53 – 10.75	(Shantanu *et al*., 2016)
2.71	2.71 – 7.75	(Dramane *et al*., 2014)
3.3	3.3 - 8.6	www.bayer.com
3.45	3.45 – 9.75	(Wei *et al*., 2014)
3.45	3.45 – 10.45	(Danielle *et al*., 2016)

2.5 Determination of cutoff score for a diagnostic test

"The cutoff value for a new diagnostic test for classifying cases as positive or negative may be determined utilizing some statistical techniques such as Mean ± 2SD and ROC curve" (Singh, 2006).

"Mean ± 2SD method (Mean ± 2-Standard-Deviation method) is the application of 95% Confidence Interval (Figure 2.2) of mean for choosing a cutoff. This method may be carried out on a sample of adequate size of diagnosed cases (known negative cases). The upper limit of its 95% Confidence Interval (i.e. mean + 2SD) may be taken as cutoff value. If a subject's test value comes greater than this cutoff value; then it may be considered positive" (Singh, 2006).
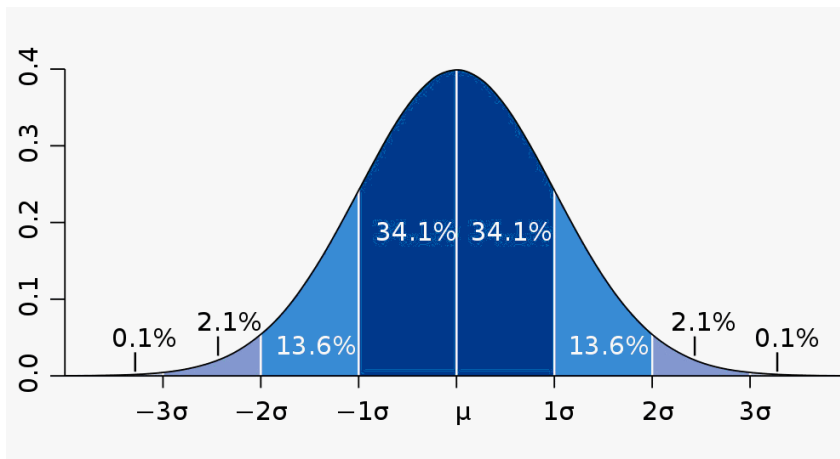
Figure 2. 2 Normal distribution curve
(https://commons.wikimedia.org/wiki/File:Standard_deviation_diagram.svg)
Assuming negative-diagnosed sample readings are normally distributed, the upper limit of
95% Confidence Interval (i.e. mean + 2SD) may be taken as cutoff value leading to 2.2%
false positivity.

"The receiver operating characteristic (ROC) curve has become a standard statistical tool to evaluate the discriminatory ability of a diagnostic test to separate diseased subjects from non-diseased subjects. For a diagnostic test with continuous scale, sensitivity (true positive rate) and specificity (true negative rate) are inversely related, in the sense that the increase of the one is accompanied with the decrease of the other as the cutoff point moves along the real number line (Figure 2.3). The ROC curve is the plot of sensitivity against (1-specificity) at all possible threshold points. A sample of adequate size may be taken with known positive and negative cases. The diagnostic test is administered and the values observed are noted. For every observed value this method displays sensitivity and (1-specificity) of the test. A particular observed value of the test may be chosen as cutoff value, which corresponds to the desired sensitivity and specificity" (Dongliang *et al*., 2017).
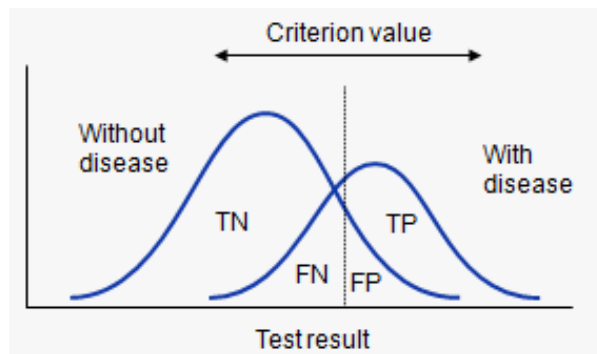
Figure 2. 3 The distribution of the test results
(https://www.medcalc.org/manual/roc-curves.php)
For a diagnostic test, as the cutoff point moves along the real number line, sensitivity (true positive rate) and specificity (true negative rate) are inversely related.

"Even though the area under the ROC curve has been widely used for measuring the accuracy of a diagnostic test, the Youden index has its unique advantage in advising an optimal cutoff for the clinicians to make diagnosis. The Youden index, is defined as the maximum of the sum of sensitivity and specificity minus one. The cutoff point, where the maximum is achieved, provides an optimal threshold for the clinicians to use the diagnostic test for classification if equal weight is placed on sensitivity and specificity. The possible values of the Youden index range from 0 to 1 with 0 indicating no discriminatory ability and 1 indicating perfect diagnostic accuracy" (Youden, 1950).

2.6 Validation of a diagnostic assay

"Test validation is a very important processes used in the laboratory to ensure that a new test performs as expected" (Robert *et al.*, 2015).

2.6.1 Analytical sensitivity

"Arguably among the most critical performance parameters for a diagnostic procedure are those related to the minimum amount of target that can

15

be detected" (Bustin *et al*., 2009). "The limit of detection (LOD), also called analytical sensitivity, is a calculated value for the lowest concentration of analyte that can be detected by the assay" (Robert *et al*., 2015). The Clinical Laboratory Standards Institute (www.clsi.org), for example, defines LoD as "the lowest amount of analyte (measurand) in a sample that can be detected with (stated) probability, although perhaps not quantified as an exact value". Nick, *et al*. (2013) state that this type of sensitivity is defined as a concentration "(e.g. as copies, cfu, pfu or genome equivalents per unit of sample material)".

"Conventionally, the LOD is reported as the estimate of the detection limit that can be achieved with 95% confidence. This determination requires Probit analysis involving testing of replicate" (Nick *et al*., 2013). "The LOD is determined by testing multiple specimens, typically 10 of each, across several dilutions (Figure 2.4). The results are then analyzed using probits (a unit of probability based on deviation from the mean of a standard deviation) and linear regression to calculate the LOD" (Robert *et al*., 2015).
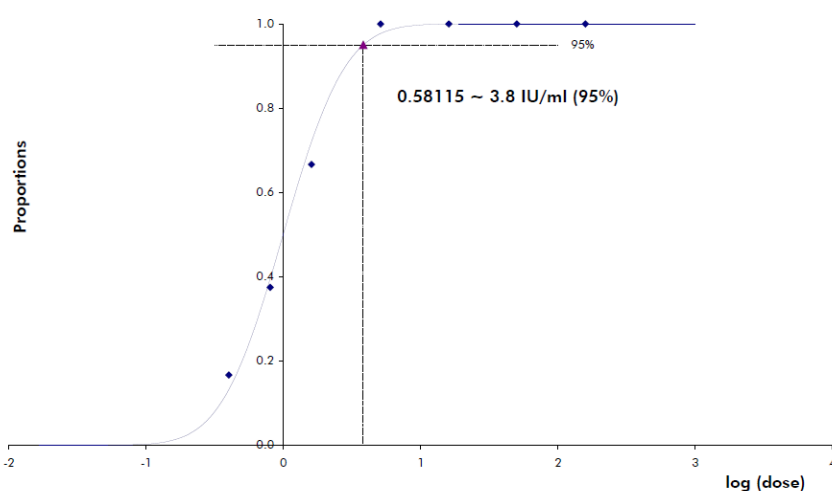
Figure 2. 4 Probit analysis: Qiagen Artus HBV PCR kit on Rotor-Gene 3000.
Conventionally, the LOD is reported as the estimate of the detection limit that can be achieved with 95% confidence which requires Probit analysis involving testing of replicate.

16

2.6.2 Anaytical specificity

Robert, *et al*. (2015) define analytical specificity as "the ability of an analytical method to detect only the analyte that it was designed to measure". "Analytical specificity is a test system parameter for laboratory-developed assays that verify that the test system does not cross-react with indigenous nucleic acid in the specimen or similar organisms. The analytical specificity is the ability of an assay to exclusively identify a target analyte or organism rather than a similar but different analyte in a specimen. Analytical specificity is determined by testing compounds with similar genetic structures, organisms that represent the normal flora of the specimen, and organisms that cause similar disease states" (Lynne, 2007).

"Analytical specificity is the ability of an assay to exclusively identify the intended target substance or organism. For validation testing should include, a wide variety of samples and strains containing the target sequence (i.e. positive in the test) as well as samples and strains containing nucleic acids that should be negative in the assay" (Nick *et al*., 2013).

2.6.3 Linear range

"The linearity of an analytical procedure is its ability to give test results which are directly proportional to the concentration of analyte. Ideally a linear relationship should be maintained across the entire range of the analytical procedure. Linearity may be assessed by testing dilutions of a quantified standard. Results should be evaluated by calculation of a regression line" (Nick *et al*., 2013).

"Results should not be extrapolated beyond the established linear dynamic range of the assay. Consequently, the quantitative range of the assay should ideally encompass the range expected from clinical samples. The standard curve should include a minimum of four points and the upper and lower values of the standards should be within 1 log of the top and bottom, respectively, of the reported quantitative range. Positive results above or below the quantitative range

should be reported appropriated (e.g. "Positive, greater than xx copies/mL" or "Positive, less than xx copies/mL" respectively)" (Nick *et al.*, 2013).

2.6.4 Precision

"Precision, or reproducibility, is a measure of the agreement between replicate analyses (using identical procedures) of a homogeneous analyte; they include inter-run, intra-run, and inter-operator variability. While the two terms are used interchangeably, historically, the term precision is generally applied to quantitative assays, while reproducibility is used with qualitative analyses" (Robert *et al.*, 2015).

"An assay may be precise but inaccurate. The precision of an analytical procedure can be expressed as the variance, standard deviation or coefficient of variation of a series of measurements. Precision can be determined by repeat testing of samples. The precision of an analytical procedure expresses the closeness of agreement between a series of measurements obtained from multiple sampling of the same homogeneous sample under prescribed conditions" (Nick *et al.*, 2013).

2.6.5 Robustness

"Robustness is a measure of the capacity of the method to remain unaffected by small variations in method parameters. The verification of the robustness allows the determination of the total failure rate of the assay. To verify the robustness, negative samples are generally spiked with quantitation standards; then, inhibitions observed and robustness of the assay is calculated" (Liesbet *et al.*, 2016).

2.6.6 Diagnostic evaluation

"The validation of clinical accuracy requires comparison of the assay to an appropriate "gold standard" method using sequential clinical samples obtained in real clinical situations. The number of samples tested will vary depending on

the availability of suitable clinical material. They should, wherever possible, include a widerange of concentrations of positive samples as well as negative samples" (Nick *et al*., 2013).

"There are a number of ways to express accuracy, but the most common is diagnostic sensitivity and specificity (formerly referred to as clinical sensitivity and specificity). The accuracy data can be displayed in a 2 x 2 table (Table 2.2)" (Lynne, 2007). "Clinical sensitivity can be expressed mathematically as a percentage of the number of true-positive results divided by the number of true-positive results plus the number of false-negative results. Clinical specificity is mathematically expressed as a percentage of the number of true-negative results divided by the number of true-negative results plus the number of false-positive results" (Robert *et al*., 2015).

Table 2. 2 Diagnostic accuracy
(https://www.medcalc.org/manual/roc-curves.php)
Diagnostic sensitivity: true-positive results divided by true-positive results plus the number of false-negative results.
Diagnostic specificity: true-negative results divided by true-negative results plus the number of false-positive results

| Test | Disease | | | | |
	Present	n	Absent	n	Total
Positive	True Positive (TP)	a	False Positive (FP)	c	a + c
Negative	False Negative (FN)	b	True Negative (TN)	d	b + d
Total		a + b		c + d	

CHAPTER 3

MATERIAL AND METHODS

3.1 Chemicals and laboratory equipment

The list of the chemicals used in the experiments is given in Appendix A (Table A.1) with their suppliers Sigma-Aldrich GmbH, Taufkirchen, Germany and Merck KGaA, Darmstadt, Germany. Basic laboratory equipment used in the experiments were Micro centrifuge-Micro CL21 (Thermo Scientific), Digital heating cooling drybath (Thermo Scientific), Precision balance (KERN), LP vortex mixer (Thermo Scientific), Mini centrifuge-mySPIN6 (Thermo Scientific), and Microwave oven (Arçelik).

3.2 Poly-glycidylmethacrylate microparticles

Poly-glycidylmethacrylate microparticles with 5 μm size and NH_2 surface functionality are purchased from Micromod Partikeltechnologie GmbH, Warnemuende, Germany. Microparticles are poly-glycidylmethacrylate particles (Figure 3.1) synthesized by dispersion polymerization. In the dispersion polymerization reaction, glycidylmethacrylate is used as monomer, benzoyl peroxide is used as initiator, ethanol is used as continuous phase, and polyacrylic acid is used as stabilizer. Ammonia activation of poly-glycidylmethacrylate particles is performed via ammonia treatment for NH_2 surface functionality (Figure 3.2).
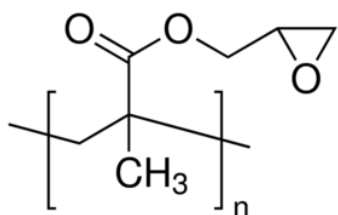
Figure 3. 1 Poly-glycidylmethacrylate microparticles
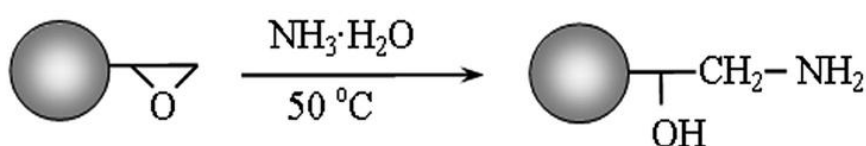
Figure 3. 2 Ammonia activation of poly-glycidylmethacrylate microparticles

3.3 PCR amplification

PCR amplification of target genes is performed with gradient thermal cycler (Arktik, 96-well gradient, Thermo Scientific, USA). Quantitative PCR kit is purchased from Qiagen GmbH, Hilden, Germany (Artus HBV PCR kit). According to the instructions in the Artus HBV PCR Kit Handbook, master mix contains reagents and enzymes for the specific amplification of a 134 bp region of the HBV genome, and oligonucleotide probes are labelled with a fluorophore that can be detected in Green Detection Channels (source: 470 nm, detector: 510 nm).

Micro particles are lyophilized onto the PCR tubes with miVac vacuum concentrator (GeneVac, SP Scientific, Missouri, USA). PCR contents and their final concentrations are given in Table 3.1 and PCR conditions are given in Table 3.2.

Table 3. 1 PCR contents and their final concentrations

PCR contents	Volume used (μl)	Final Concentration
PCR Master mix	30	-
Template (50 pg/μl)	20	5-10 pg/μl
Micro-particles	-	5-40 μg/μl
Total Volume	**50**	

Table 3. 2 PCR conditions

Temperature (ºC)	Time (sec.)	Cycle number	Steps
95	600	1	Initial denaturation
95	15		Denaturation
55	30	45	Annealing
72	15		Extension

After PCR, the products were analyzed by agarose gel electrophoresis using Electrophoresis System, Easy-Cast Horizontal Minigel and Power Supply, Thermo Scientific. Molecular imaging is performed with Gel Documentation System, Doc-print vX5, Vilber Lourmat.

3.4 Prototype manufacturing

Prototype device was manufactured using the equipment listed below:

1. CNC (Computer Numerical Control) vertical processing center, DMU50 5 axis 500x450x400, Deckhel Maho
2. Laser cutting profile machine, Space Gear MK II, Mazak
3. Press brake machine, 12250KG, Durmazlar
4. Laser engraving machine, HS-K6040, Foshan

5. Metal band saw machine, Baykal

6. Tapping machine, Cetinkaya

7. Drill press, Heltos

8. Air tool, 600 WATT-12000-27000 MIN-1, Bosch

9. TIG welder, Lincoln

10. Angle grinder, Bosch

3.5 Image Analysis

Image analysis was performed using Kodak 1D Image Analysis Software provided by Kodak ImageStation 2000MM system (Eastman Kodak Company, New Haven, USA). Using the ROI (region of interest) function of the software, regions of interest (ROIs) were defined using a standard area for each sample. The mean ROI intensities were expressed with arbitrary units as the sum of background-subtracted pixel intensity values devided by total pixels in the standard area within the ROI.

3.6 Statistical Analysis

Mean and standard deviation of fluorescence intensity readings of negative samples are calculated with Microsoft Excel Software. Analytical sensitivity was analyzed by use of a dilution series of Quantitation Standard (Artus, Qiagen, Germany), and limit of detection was determined by probit analysis and by curve fitting using Microsoft Excel Software.

Pearson's correlation coefficient was used to assess the strength of the linear association between the log-transformed values of the assay and reference methods. To compare results obtained by two different methods, the fitted regression lines were compared with the line of equality by testing the two-tailed hypothesis of slope=1 and intercept=0. The coefficient of variation was calculated for samples quantified in repeated measurements with Microsoft Excel Software.

CHAPTER 4

RESULTS AND DISCUSSION

4.1 Decreasing PCR background fluorescence

An HBV positive diagnosed and an HBV negative diagnosed sample has been analysed with PCR in presence of oligonucleotide probes (first and second PCR tubes from left to right; Figure 4.1) and in the presence of both oligonucleotide probes and microparticles (third and fourth PCR tubes from left to right; Figure 4.1). PCR amplification of target genes is performed with gradient thermal cycler (Arktik, 96-well gradient, Thermo Scientific, USA) using Artus HBV PCR kit (Qiagen GmbH, Germany). According to the instructions in the Artus HBV PCR Kit Handbook, master mix contains reagents and enzymes for the specific amplification of a 134 bp region of the HBV genome, and oligonucleotide probes are labelled with a fluorophore that can be detected in Green Detection Channels (source: 470 nm, detector: 510 nm). Microparticles are lyophilized onto the PCR tubes to have a final concentration of 40 µg/µl (third and fourth PCR tubes from left to right; Figure 4.1). Amplification was carried out in a total of 50 µl reaction mix containing 30 µl PCR Master Mix and 20 µl template DNA. PCR contents and their final concentrations are given in Table 4.1 and PCR conditions are given in Table 4.2.
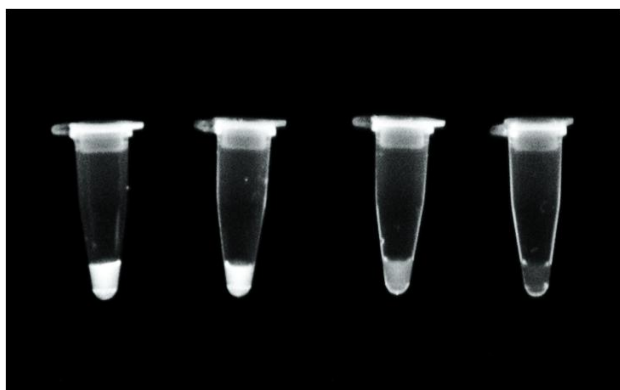
Figure 4. 1 Reducing PCR background fluorescence

An HBV positive diagnosed and an HBV negative diagnosed sample has been analysed with quantitative PCR (first and second tubes from left to right) and microparticle based PCR (third and fourth tubes from left to right). Fluorescence intensity difference between third sample from left to right and fourth sample from left to right is visible to human eye.

Table 4. 1 PCR contents and their final concentrations

PCR contents	Volume used (μl)	Final Concentration
PCR Master mix	30	-
Template (50 pg/μl)	20	5-10 pg/μl
Micro-particles	-	40 μg/μl
Total Volume	**50**	

Table 4. 2 PCR conditions

Temperature (°C)	Time (sec.)	Cycle number	Steps
95	600	1	Initial denaturation
95	15		Denaturation
55	30	45	Annealing
72	15		Extension

After PCR, the products were analyzed by agarose gel electrophoresis (Figure 4.2) using Electrophoresis System, Easy-Cast Horizontal Minigel and Power Supply, Thermo Scientific. Molecular imaging is performed with Gel Documentation System, Doc-print vX5, Vilber Lourmat.

Figure 4. 2 PCR verification by agarose gel electrophoresis
M: 100 bp molecular weight marker, Lane1: HBV positive diagnosed sample analysed with quantitative PCR, Lane2: HBV negative diagnosed sample analysed with quantitative PCR, Lane3: HBV positive diagnosed sample analysed with microparticle based PCR, Lane4: HBV negative diagnosed sample analysed with microparticle based PCR.

Oligonucleotide probes that are unused in PCR adsorb onto the micro particles; however, fluorophore molecules released with the exo-nuclease activity of *Taq.* DNA polymerase does not adsorb onto micro particles. By this way,

27

background fluorescence is reduced and the need for sensitive sensors for detecting the fluorescence difference disappears (Figure 4.1).

Existing image analysis systems with highly sensitive sensors may diagnose first sample from left to right to be positive and second sample from left to right to be negative (Figure 4.1). On the other hand, with the use of microparticles, fluorescence intensity difference between third sample from left to right and fourth sample from left to right is visible to human eye without any need for sensitive sensors (Figure 4.1). Therefore, a cost-friendly prototype diagnostic device is designed, manufactured and validated.

4.2 Prototype manufacturing
4.2.1 Light source, CCD camera and filters

A low-cost CCD (charge-coupled device) camera was purchased from Sony Corporation (38x38 mm, working temperature: -10°C / +50°C, working humidity: 20 to 80%). A low-cost light source was purchased from Troy-CSL Lighting, Inc. (3xAAA battery, 1000 Lumen). Excitation band-pass filters (490 nm and 650 nm wavelength) and emission band-pass filters (520 nm and 670 nm wavelength) were purchased from Newport Corporation (Figure 4.3).

Figure 4. 3 Light source, CCD camera and filters

4.2.2 Technical drawings for prototype device

Prototype device is intended to be used in clinical diagnostics. For this reason, prototype device was designed to be in conformity with related standards: ISO 13485:2012 Medical devices - Quality management systems - Requirements for regulatory purposes, and ISO 14971:2012 Medical devices - Application of risk management to medical devices. Technical drawing for prototype device including a LED (light emitting diode) light source, an excitation band-pass filter (490 nm), a sample carousel, an emission band-pass filter (520 nm) and a CCD (charge-coupled device) camera is given in Figure 4.4.
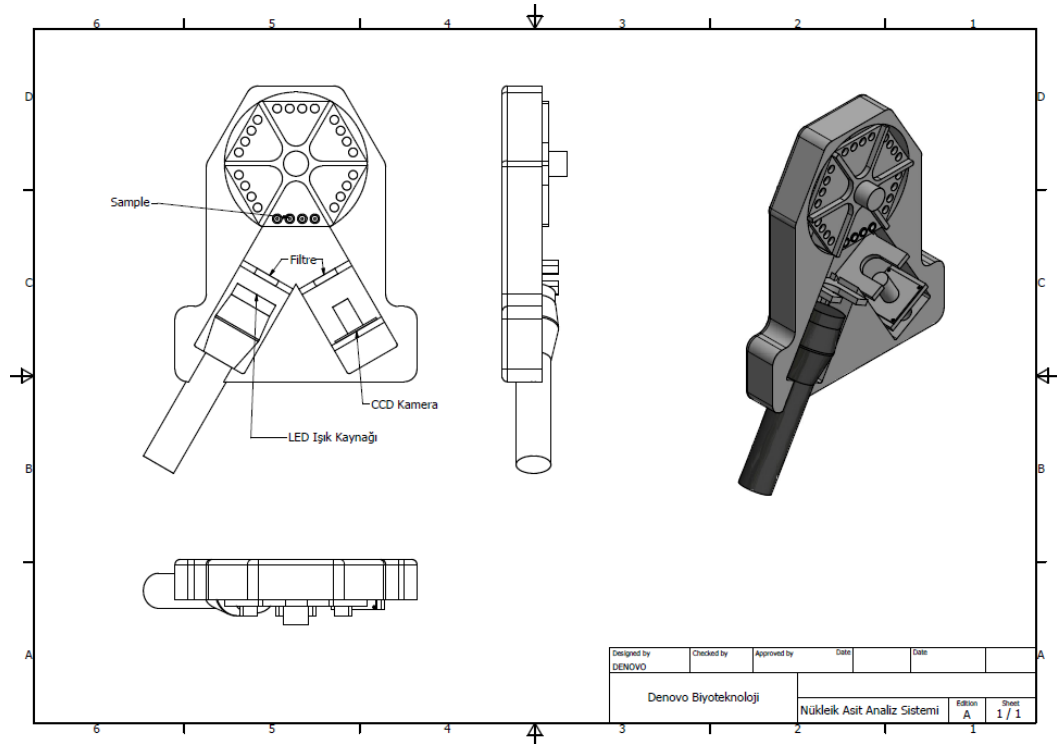
Figure 4. 4 Technical drawing for prototype device

4.2.3 Sample carousel design

Sample carousel was designed for analysis of 24 samples at a time. Sample carousel design is given in Figure 4.5. 3D illustration of prototype device is given in Figure 4.6.
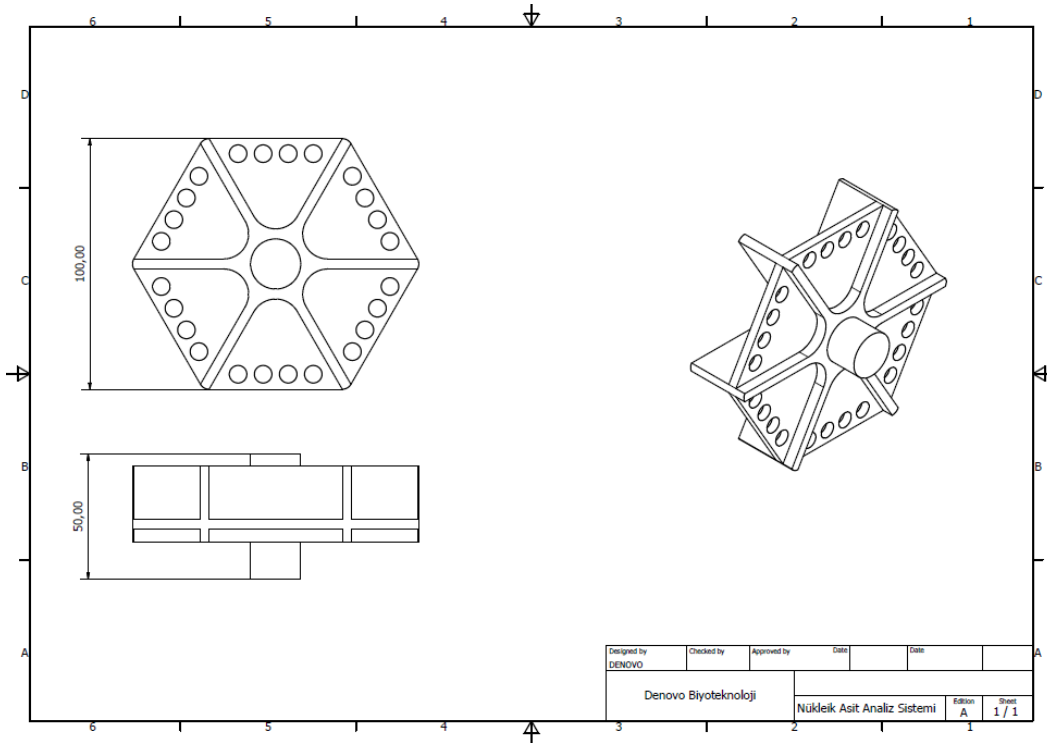
Figure 4. 5 Sample carousel design
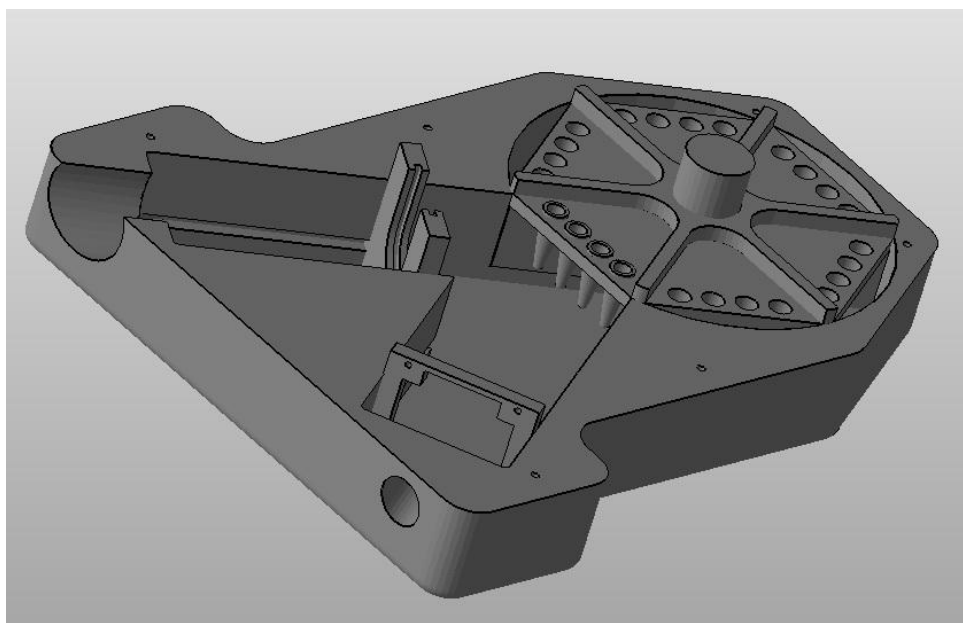
Figure 4. 6 3D illustration of prototype device

4.2.4 Manufacturing prototype

Prototype device including a LED (light emitting diode) light source, two filter sliders, two excitation band-pass filters (490 nm and 650 nm wavelength), a 24 sample carousel, two emission band-pass filters (520 nm and 670 nm wavelength), and a CCD (charge-coupled device) camera was manufactured with a cost of 500 € (Figure 4.7 – 4.12).

Prototype is manufactured (Figure 4.7) and filters (using filter sliders), light source, and CCD camera are installed (Figure 4.8). LED light source, filters and CCD camera are properly fixed into their locations and CCD camera settings are optimized in order to ensure standardization in fluorescence intensity readings. Inition illumination testing was carried out (Figure 4.9).

With the manufactured prototype, samples are excited with the light filtered by excitation filters and emission from the samples is filtered by emission filters through the camera.
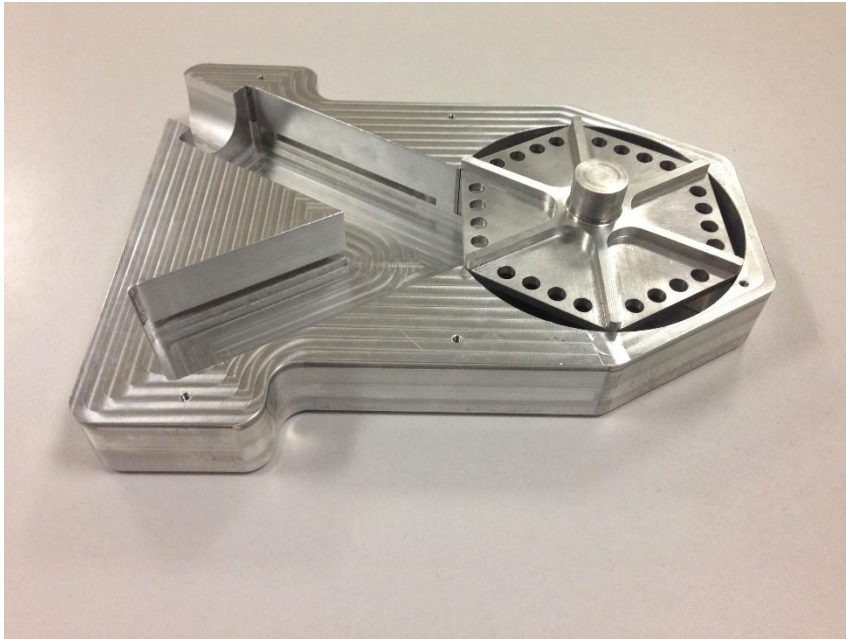
Figure 4. 7 Manufacturing prototype
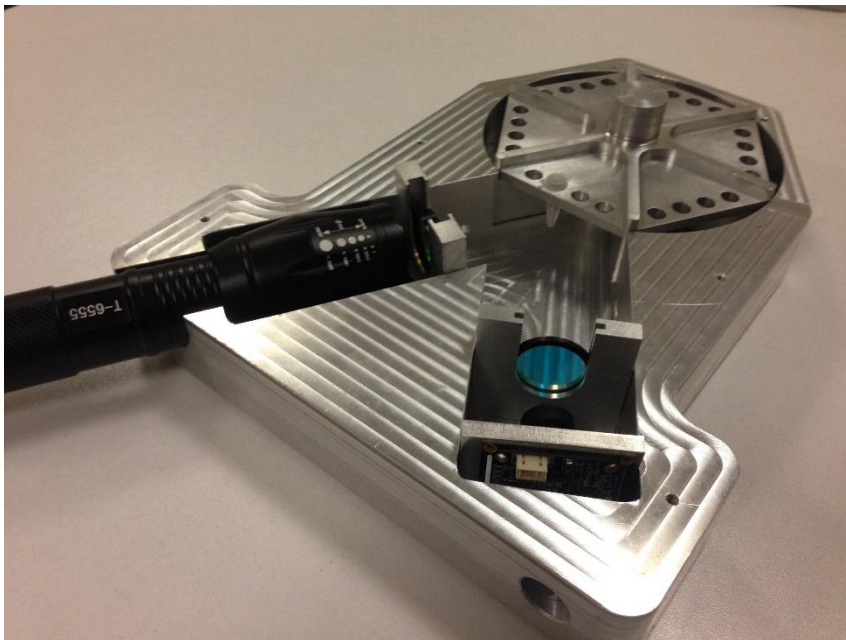
Figure 4. 8 Installation of light source, CCD camera and filters

Figure 4. 9 Initial testing of the prototype

4.2.5 Light-proof lid design and black finishing

The lid of the prototype is designed to be light-proof (Figure 4.10). In order to avoid reflection, black finishing is applied onto the prototype device (Figure 4.11). Finally, prototype device including a LED (light emitting diode) light source, two filter sliders, two excitation band-pass filters (490 nm and 650 nm wavelength), a 24 sample carousel, two emission band-pass filters (520 nm and 670 nm wavelength), and a CCD (charge-coupled device) camera was manufactured with a cost of 500 € (Figure 4.12).
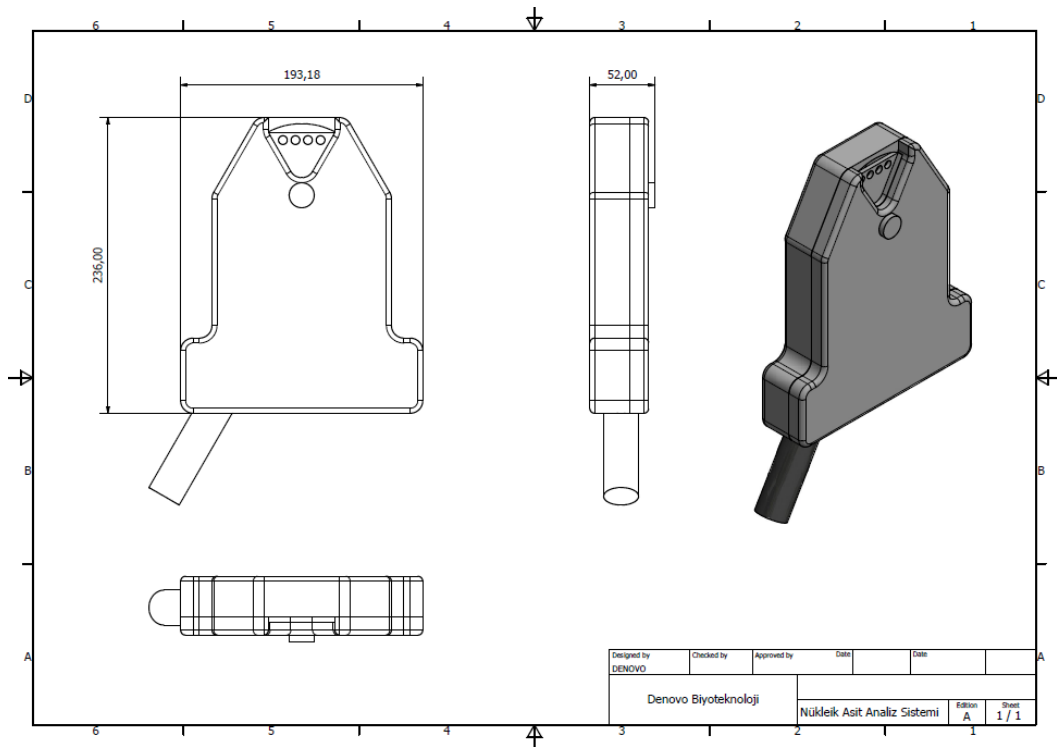
Figure 4. 10 Light-proof lid design
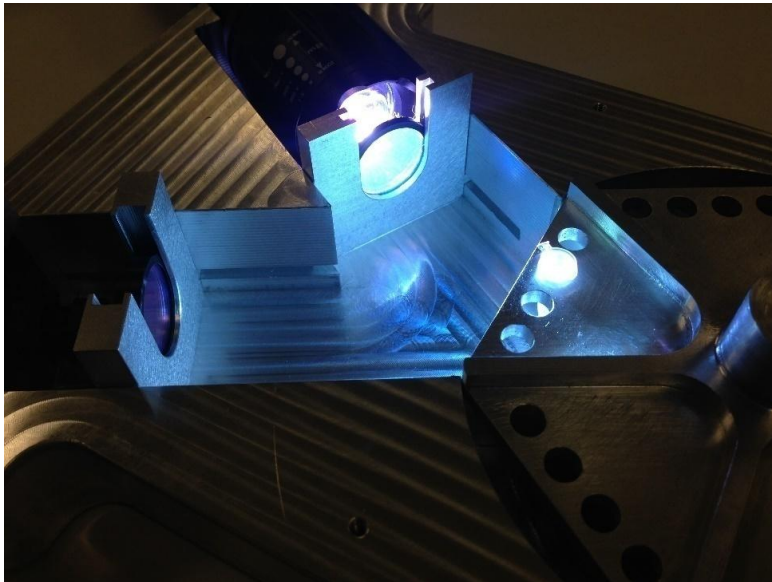
Figure 4. 11 Black finishing

Figure 4. 12 Image of manufactured prototype

4.2.6 Prototype design output

An HBV positive diagnosed and an HBV negative diagnosed sample has been analysed with PCR in presence of oligonucleotide probes (first and second PCR tubes from left to right; Figure 4.13) and in the presence of both oligonucleotide probes and microparticles (third and fourth PCR tubes from left to right; Figure 4.13). PCR amplification of target genes is performed with gradient thermal cycler (Arktik, 96-well gradient, Thermo Scientific, USA) using Artus HBV PCR kit (Qiagen GmbH, Germany). According to the instructions in the Artus HBV PCR Kit Handbook, master mix contains reagents and enzymes for the specific amplification of a 134 bp region of the HBV genome, and oligonucleotide probes are labelled with a fluorophore that can be detected in Green Detection Channels (source: 470 nm, detector: 510 nm). Microparticles are

lyophilized onto the PCR tubes to have a final concentration of 40µg/µl (third and fourth PCR tubes from left to right; Figure 4.13). Amplification was carried out in a total of 50 µl reaction mix containing 30 µl PCR Master Mix and 20 µl template DNA. PCR contents and their final concentrations are given in Table 4.3 and PCR conditions are given in Table 4.4. Image analysis was performed using Kodak 1D Image Analysis Software provided by Kodak ImageStation 2000MM system (Eastman Kodak Company, New Haven, USA). Using the ROI (region of interest) function of the software, regions of interest (ROIs) were defined using a standard area for each sample. The mean ROI intensities were expressed with arbitrary units as the sum of background-subtracted pixel intensity values devided by total pixels in the standard area within the ROI.
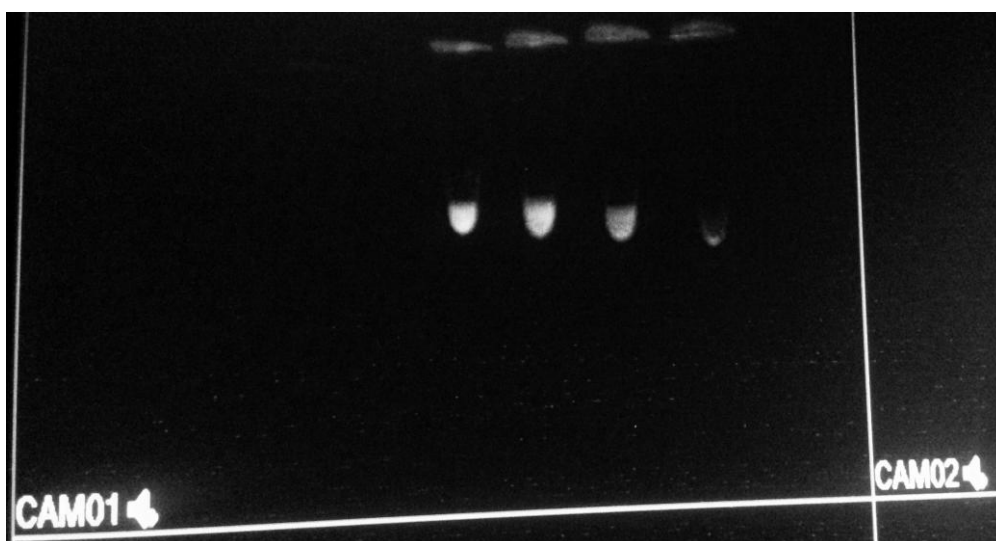
Figure 4. 13 Prototype image; reducing PCR background fluorescence
An HBV positive diagnosed and an HBV negative diagnosed sample has been analysed with quantitative PCR (first and second tubes from left to right and microparticle based PCR (third and fourth tubes from left to right). In the image captured with prototype, fluorescence intensity difference between third sample from left to right and fourth sample from left to right is visible to human eye without any need for sensitive sensors.

Table 4. 3 PCR contents and their final concentrations

PCR contents	Volume used (µl)	Final Concentration
PCR Master mix	30	-
Template (50 pg/µl)	20	5-10 pg/µl
Micro-particles	-	40 µg/µl
Total Volume	**50**	

Table 4. 4 PCR conditions

Temperature (ºC)	Time (sec.)	Cycle number	Steps
95	600	1	Initial denaturation
95	15		Denaturation
55	30	45	Annealing
72	15		Extension

After PCR, the products were analyzed by agarose gel electrophoresis (Figure 4.14) using Electrophoresis System, Easy-Cast Horizontal Minigel and Power Supply, Thermo Scientific. Molecular imaging is performed with Gel Documentation System, Doc-print vX5, Vilber Lourmat.
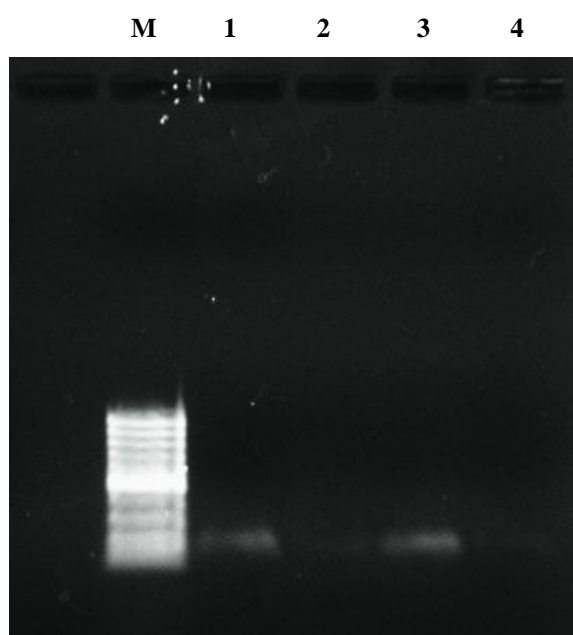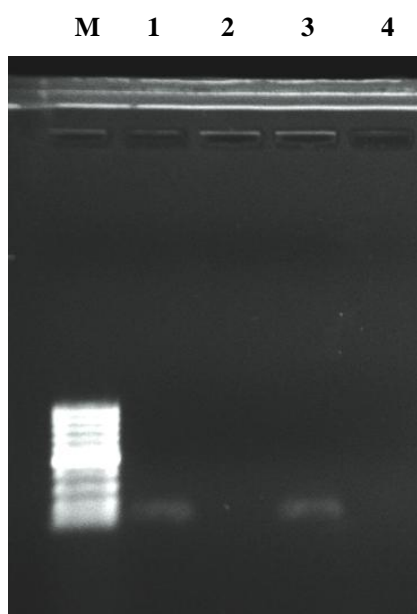
Figure 4. 14 PCR verification with agarose gel electrophoresis
M: 100 bp molecular weight marker, Lane1: HBV positive diagnosed sample analysed with quantitative PCR, Lane2: HBV negative diagnosed sample analysed with quantitative PCR, Lane3: HBV positive diagnosed sample analysed with microparticle based PCR, Lane4: HBV negative diagnosed sample analysed with microparticle based PCR.

Oligonucleotide probes that are unused in PCR adsorb onto the micro particles; however, fluorophore molecules released with the exo-nuclease activity of *Taq.* DNA polymerase does not adsorb onto micro particles. By this way, background fluorescence is reduced and the need for sensitive sensors for detecting the fluorescence difference disappears (Figure 4.13).

Existing image analysis systems with highly sensitive sensors may diagnose first sample from left to right to be positive and second sample from left to right to be negative (Figure 4.13). On the other hand, with the use of microparticles, fluorescence intensity difference between third sample from left to right and fourth sample from left to right is visible to human eye without any need for sensitive sensors (Figure 4.13).

4.3 Microparticle optimization

An HBV negative diagnosed sample has been analysed with PCR in presence of oligonucleotide probes and in presence of both oligonucleotide probes and microparticles. PCR amplification of target genes is performed with gradient thermal cycler (Arktik, 96-well gradient, Thermo Scientific, USA) using Artus HBV PCR kit (Qiagen GmbH, Germany).

Microparticles are lyophilized onto PCR tubes to have desired concentrations in the range 0-40 µg/µl after the addition of PCR master mix and DNA sample.

Amplification was carried out in a total of 50 µl reaction mix containing 30 µl PCR Master Mix and 20 µl template DNA. PCR contents and their final concentrations are given in Table 4.5 and PCR conditions are given in Table 4.6. Image analysis was performed using Kodak 1D Image Analysis Software provided by Kodak ImageStation 2000MM system (Eastman Kodak Company, New Haven, USA). Using the ROI (region of interest) function of the software, regions of interest (ROIs) were defined using a standard area for each sample. The mean ROI intensities were expressed with arbitrary units as the sum of background-subtracted pixel intensity values devided by total pixels in the standard area within the ROI.

Table 4. 5 PCR contents and their final concentrations

PCR contents	Volume used (µl)	Final Concentration
PCR Master mix	30	-
Template (50 pg/µl)	20	5-10 pg/µl
Micro-particles	-	0-40 µg/µl
Total Volume	**50**	

Table 4. 6 PCR conditions

Temperature (°C)	Time (sec.)	Cycle number	Steps
95	600	1	Initial denaturation
95	15		Denaturation
55	30	45	Annealing
72	15		Extension

Initial liquid phase probe concentration (pmol/µl) [C^0_{Pro}] and liquid phase probe concentration (pmol/µl) [C_{Pro}] were calculated by mass balance using fluorescence intensity readings. Solid phase (adsorbed) probe concentration per total probe concentration [$(C^0_{Pro}-C_{Pro})/C^0_{Pro}$] versus particle concentration (µg/µl) [$C_{particle}$] graph is plotted (Figure 4.15; data given in Appendix B, Table B.1). Microparticle concentration of 30 µg/µl is chosen for reducing PCR background fluorescence.
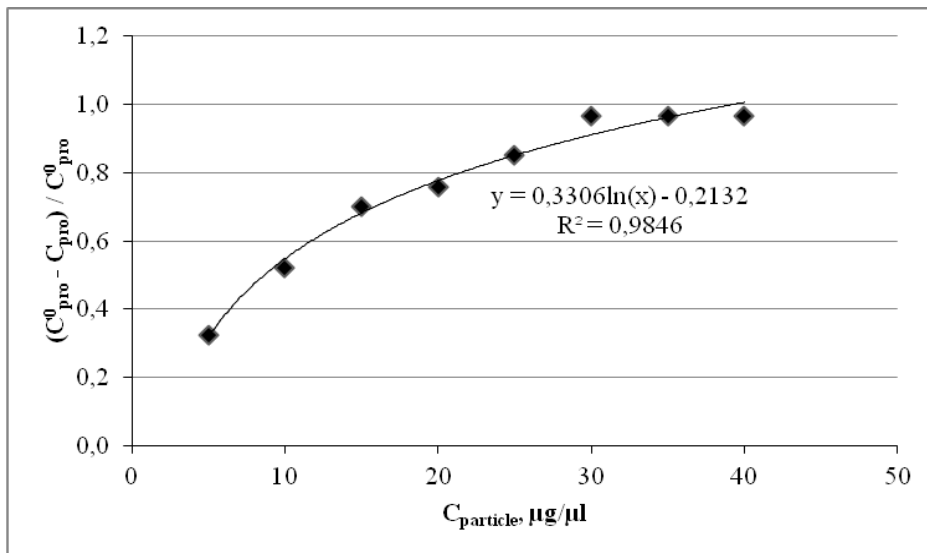
Figure 4. 15 Microparticle optimization

4.3.1 Adsorption isotherms and constants

Equilibrium based adsorption analysis is performed by using the measured liquid and solid phase solute (probe) equilibrium concentrations. Adsorption isotherm is plotted (Figure 4.16; data given in Appendix B, Table B.2). The isotherm best fits in linear type isotherm (Figure 4.17).

Most isotherms are linear when the solute concentration is very low. The linear isotherm is given by:

$$q = Ky \qquad (4.1)$$

where q is the amount of solute adsorbed per amount of adsorbent, y is the solute concentration in solution, and K is linear equilibrium constant. Linear equilibrium constant is the slope of the fitted line;

$$K = 0.0532 \ (pmol_{solid} \ / \ \mu g \ particle) \ / \ (pmol_{liquid} \ / \mu l) \qquad (4.2)$$

Calculated linear equilibrium constant may be useful for estimating microparticle concentration for different PCR total volumes.
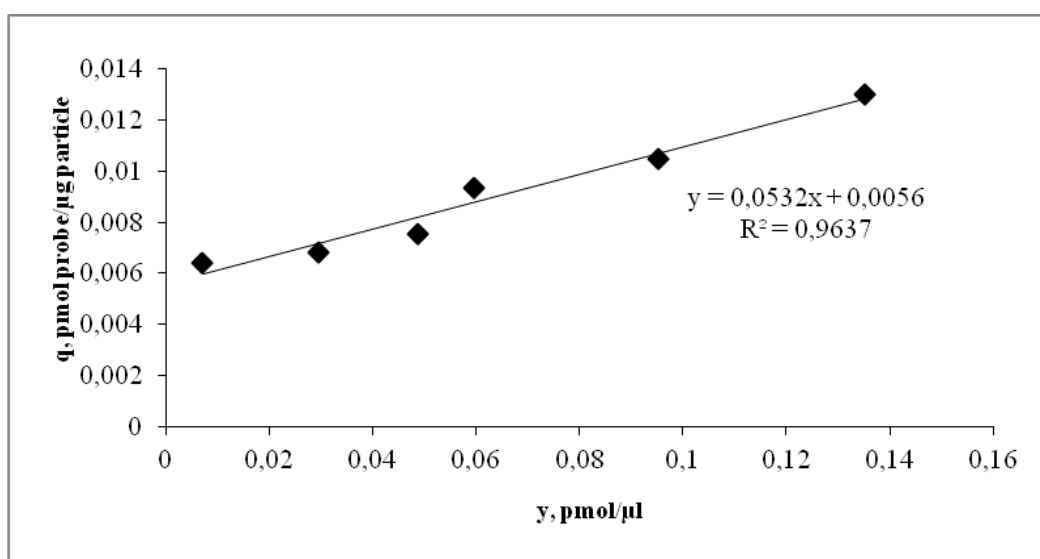
Figure 4. 16 Adsorption isotherm
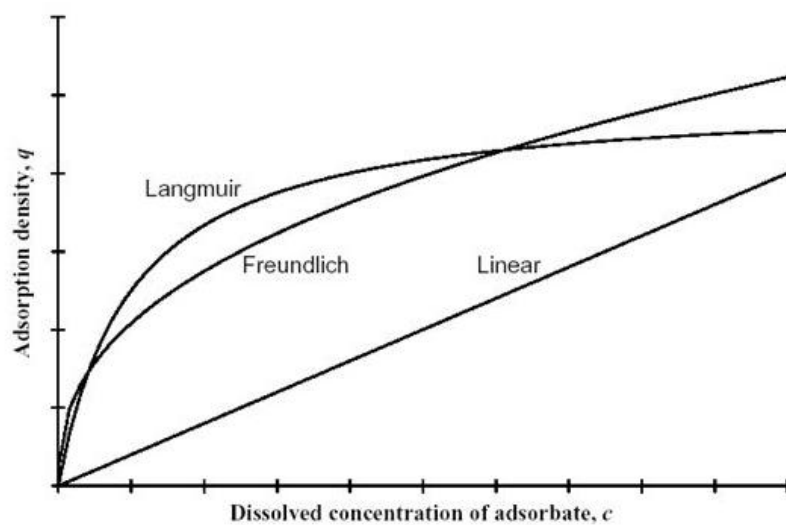
Figure 4. 17 Langmuir, Freundlich, and Linear type adsorption isotherms
(https://www.slideshare.net/alexmpharm/adsorption-50461077)

42

4.4 Validation of diagnostic test and prototype

In validation study, HBV negative and HBV positive diagnosed samples have been analysed with PCR in presence of both oligonucleotide probes and microparticles. PCR amplifications of target genes are performed with gradient thermal cycler (Arktik, 96-well gradient, Thermo Scientific, USA) using Artus HBV PCR kit (Qiagen GmbH, Germany). Microparticles are lyophilized onto the PCR tubes to have a final concentration of 30 µg/µl. Amplifications were carried out in a total of 50 µl reaction mix containing 30 µl PCR Master Mix and 20 µl template DNA. PCR contents and their final concentrations are given in Table 4.7 and PCR conditions are given in Table 4.8. Image analysis was performed using Kodak 1D Image Analysis Software provided by Kodak ImageStation 2000MM system (Eastman Kodak Company, New Haven, USA). Using the ROI (region of interest) function of the software, regions of interest (ROIs) were defined using a standard area for each sample. The mean ROI intensities were expressed with arbitrary units as the sum of background-subtracted pixel intensity values devided by total pixels in the standard area within the ROI.

Table 4. 7 PCR contents and their final concentrations

PCR contents	Volume used (µl)	Final Concentration
PCR Master mix	30	-
Template (50 pg/µl)	20	5-10 pg/µl
Micro-particles	-	30 µg/µl
Total Volume	**50**	

Table 4. 8 PCR conditions

Temperature (°C)	Time (sec.)	Cycle number	Steps
95	600	1	Initial denaturation
95	15		Denaturation
55	30	45	Annealing
72	15		Extension

4.4.1 Determination of cutoff score for diagnostic test

The cutoff value for diagnostic test for classifying cases as positive and negative is determined utilizing Mean ± 2SD and ROC curve methods.

In Mean ± 2SD method, prototype fluorescence intensity readings of DNA eluates from 105 HBV negative-diagnosed and 187 HBV positive-diagnosed samples are recorded (Appendix B, Table B.3). Mean of fluorescence intensity readings of negative samples are calculated as 26.00. Standard deviation (SD) of fluorescence intensity readings of negative samples are calculated as 0.52. The upper limit of 95% Confidence Interval (mean + 2SD) is calculated as 27.04. This value is the first candidate for cutoff score.

In ROC curve method, taking each fluorescence intensity reading as cutoff value, sensitivity (true positive rate) and specificity (true negative rate) of the test is calculated, and candidate cutoff values are investigated (Table 4.9).

The Youden index, is defined as the maximum of the sum of sensitivity and specificity minus one. The cutoff point, where the maximum is achieved, provides an optimal threshold for the clinicians to use the diagnostic test for classification if equal weight is placed on sensitivity and specificity (Youden, 1950).

At 27.45, maximum of the sum of sensitivity and specificity minus one is achieved: 0.979 (Table 4.9). This value is the second candidate for cutoff score. If the first candidate (27.04) is set to be cutoff, sum of sensitivity and specificity

minus 1 is calculated as 0.959. Since 0.959 is lower than 0.979, cutoff value is determined to be 27.45.

The possible values of the Youden index range from 0 to 1 with 0 indicating no discriminatory ability and 1 indicating perfect diagnostic accuracy (Youden, 1950). At the cutoff point (27.45), Youden Index (=0.979) is close to 1 indicating high diagnostic accuracy.

In this study, prototype fluorescence intensity readings of DNA eluates from 105 HBV negative-diagnosed and 187 HBV positive-diagnosed samples are recorded. The readings scatter in a relatively large range; the readings range between 24.67 and 200.98. However, the readings of negative-diagnosed and positive-diagnosed samples overlap in a narrow range (25.42 - 27.45). In this narrow range, if fluorescent intensity readings 26.90 and 26.93 are chosen as cutoff score, different spesificities (0.952 and 0.962, respectively) are obtained (Table 4.9). Thus, rounding fluorescent intensity reading 26.93 to 26.9 is not convenient in this assay. In this study, in order to avoid false positivities and false negativities, two digits after decimal point were decided to be significant in fluorecence intensity readings.

Table 4. 9 Youden index analysis

Fluorescence Intensity	Sensitivity	Specificity	Sum of (sensitivity+ specificity-1)
…	…	…	…
26.9	0.979	0.952	0.931
26.93	0.979	0.962	0.940
26.97	0.979	0.971	0.950
27.12	0.979	0.981	0.959
27.32	0.979	0.990	0.969
25.42	1.000	0.135	0.135
25.93	0.995	0.452	0.447
26.18	0.989	0.644	0.634
26.69	0.984	0.894	0.878
27.45	**0.979**	**1.000**	**0.979**
28.72	0.973	1.000	0.973
30.74	0.968	1.000	0.968
…	…	…	…

4.4.2 Analytical sensitivity

Analytical sensitivity was analyzed by use of a dilution series of Quantitation Standard (Artus, Qiagen, Germany), and limit of detection was determined by probit analysis and validated by curve fitting using Microsoft Excel Software. Probit analysis is a type of regression used to analyze binomial response variables. Probit analysis is a standard, robust, empirical method for determining Quantitative PCR LODs that is commonly used in clinical microbiology.

A dilution series of HBV Quantitation Standard was prepared to give the final $\log_{10}$ concentrations of 2.35, 2.25, 2.15, 2.12, 2.10, 2.08, 2.05, 2.02, 2.00, 1.95, 1.85, and 1.75 copy/ml. Each dilution was tested in 24 replicates (3 different days on 8 replicates) (Data given in Appendix B, Table B.4). The results were determined by a probit analysis and validated by curve fitting.

In probit analysis, tested concentrations, the number of samples per concentration that responded, and the total number of samples tested per concentration are listed (Table 4.10) and a graph of responding (%) versus $\log_{10}$ concentration (copy/ml) was plotted (Figure 4.18). The sigmoid dose-response curve (Figure 4.18) is converted to a straight line (Figure 4.19) by probit analysis and LOD is determined with regression analysis.

Table 4. 10 Probit analysis

Log_{10} concentration	Samples responded	Total samples	Responding (%)
2.35	24	24	100
2.25	24	24	100
2.15	24	24	100
2.12	24	24	100
2.10	23	24	95.8
2.08	21	24	87.5
2.05	13	24	54.2
2.02	7	24	29.2
2.00	3	24	12.5
1.95	0	24	0
1.85	0	24	0
1.75	0	24	0
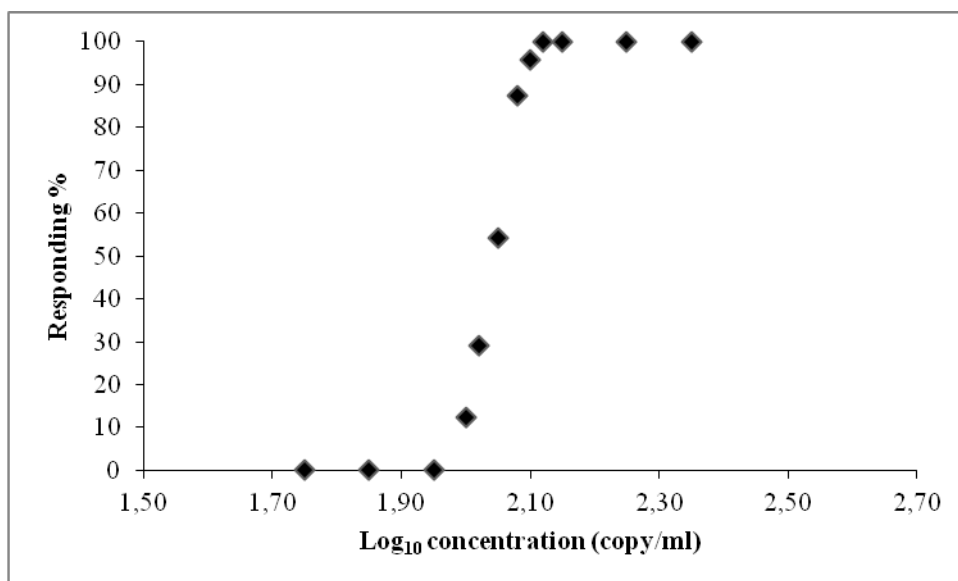
Figure 4. 18 Sigmoid dose-response curve

In order to convert the sigmoid dose-response curve (Figure 4.18) to straight line, the percentage responding at each concentration are transformed to probits, a measure of detection probability (short for "probability units"). Probits are determined by looking up those corresponding to the % responded in Finney's table (Finney, 1952) (Table 4.11). At each $\log_{10}$ concentration, responding(%) is converted to probits (Table 4.12).

Table 4. 11 Transformation of percentages to probits

(Finney, 1952)

%	0	1	2	3	4	5	6	7	8	9
0	—	2.67	2.95	3.12	3.25	3.36	3.45	3.52	3.59	3.66
10	3.72	3.77	3.82	3.87	3.92	3.96	4.01	4.05	4.08	4.12
20	4.16	4.19	4.23	4.26	4.29	4.33	4.36	4.39	4.42	4.45
30	4.48	4.50	4.53	4.56	4.59	4.61	4.64	4.67	4.69	4.72
40	4.75	4.77	4.80	4.82	4.85	4.87	4.90	4.92	4.95	4.97
50	5.00	5.03	5.05	5.08	5.10	5.13	5.15	5.18	5.20	5.23
60	5.25	5.28	5.31	5.33	5.36	5.39	5.41	5.44	5.47	5.50
70	5.52	5.55	5.58	5.61	5.64	5.67	5.71	5.74	5.77	5.81
80	5.84	5.88	5.92	5.95	5.99	6.04	6.08	6.13	6.18	6.23
90	6.28	6.34	6.41	6.48	6.55	6.64	6.75	6.88	7.05	7.33
—	0.0	0.1	0.2	0.3	0.4	0.5	0.6	0.7	0.8	0.9
99	7.33	7.37	7.41	7.46	7.51	7.58	7.65	7.75	7.88	8.09

Table 4. 12 Transformation of percentages to probits

Log_{10} concentration	Responding (%)	Probits
2.35	100	8.09
2.25	100	8.09
2.15	100	8.09
2.12	100	8.09
2.10	95.8	6.73
2.08	87.5	6.16
2.05	54.2	5.11
2.02	29.2	4.46
2.00	12.5	3.84
1.95	0	-
1.85	0	-
1.75	0	-

A graph of the probits versus the $\log_{10}$ of the concentrations is plotted (Figure 4.19). The relationship between probits and $\log_{10}$ concentrations is linear. Linear regression analysis comparing the probits-versus-$\log_{10}$ concentration was as follows:

$$\text{Probits} = 33.132 \text{ x } (\log_{10} \text{ concentration}) - 62.575 \tag{4.3}$$
with a correlation coefficient (R^2) of 0.9694.

Line of regression is fitted to determine the C_{95} (95% responding concentration) by searching the Finney's table (Finney, 1952) for a probit of 9.50 (probit for 95% is 6.64).

The 95% limit of detection $\log_{10}$ concentration is calculated as 2.09 copy/ml. This means that there is a 95% probability that $\log_{10}$ concentration of 2.09 copy/ml will be detected.
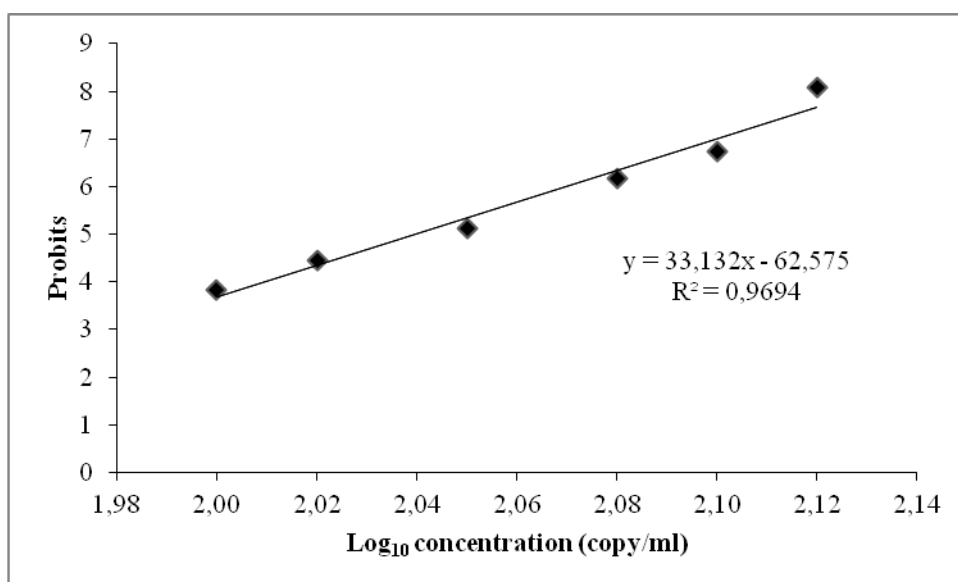
Figure 4. 19 Calculation of limit of detection (LOD)

In order to validate the result obtained with probit analysis, curve fitting analysis was applied for sigmoid dose-response curve (Figure 4.18). The relationship between responding (%) and $\log_{10}$ concentrations was as follows:

$$\text{Responding (\%)} = 1 / (1 + e^{(44.123 - 21.625\,\log_{10}\,\text{concentration})}) \quad (4.4)$$

By curve fitting, the 95% limit of detection $\log_{10}$ concentration is calculated as 2.10 copy/ml. By probit analysis, the 95% limit of detection $\log_{10}$ concentration was calculated as 2.09 copy/ml. Therefore, the result obtained with probit analysis is validated with curve fitting method. Probit analysis is recommended by the Clinical and Laboratory Standards Institute for determining the 95% LOD (CLSI, 2012) and probit analysis is extensively applied in determination the 95% LOD in commercial assays; therefore, the 95% limit of detection $\log_{10}$ concentration is determined as 2.09 copy/ml. This means that there is a 95% probability that $\log_{10}$ concentration of 2.09 copy/ml will be detected. Comparison of limit of detection result of the current study with published studies and commercial assays for HBV diagnosis is given in Table 4.13.

Table 4. 13 Comparison of limit of detection result of the current study with published studies and commercial assays for HBV diagnosis

Limit of detection (log$_{10}$ concentration copy/ml)	Linear range (log$_{10}$ concentration copy/ml)	Source
2.02	2.02 – 8.92	www.roche.com
2.05	2.05 – 11.75	www.qiagen.com
2.09	**2.09 – 8.75**	**this thesis**
2.13	2.13 – 11.13	(Garson *et al.*, 2005)
2.14	2.14 – 9.75	www.rtalabs.com.tr
2.17	2.17 – 8.17	www.abbott.com
2.39	2.39 – 10.39	(Kavita *et al.*, 2006)
2.4	2.4 – 11.4	(Paraskevis *et al.*, 2002)
2.53	2.53 – 10.75	(Shantanu *et al.*, 2016)
2.71	2.71 – 7.75	(Dramane *et al.*, 2014)
3.3	3.3 – 8.6	www.bayer.com
3.45	3.45 – 9.75	(Wei *et al.*, 2014)
3.45	3.45 – 10.45	(Danielle *et al.*, 2016)

4.4.3 Analytical specificity

The analytical specificity was validated with 105 different HBV negative-diagnosed samples (Appendix B, Table B.3). None of the HBV negative clinical specimens gave positive test result for HBV DNA. Cross-reactivity study was performed for potential cross-reactive markers. The analytical specificity of the assay was evaluated by testing 18 reference organisms with 18 clinical specimens which were positive. A potential cross-reactivity was tested using the control group listed in Table 4.14. None of the tested pathogens has been reactive.

Table 4. 14 Analytical specificity

Sample Number	Known Qualitative Diagnosis (+/-)	Prototype Fluorescence Intensity	Prototype Qualitative Analysis (+/-)
HSV1	-	24.92	-
HSV2	-	25.88	-
EBV	-	25.93	-
CMV	-	25.01	-
HIV1	-	26.04	-
HAV	-	25.21	-
HCV	-	26.11	-
E.coli	-	26.19	-
MT	-	25.52	-
HPV16	-	26.25	-
TTV	-	25.56	-
HHV8	-	26.34	-
HHV6	-	25.61	-
H.pylori	-	26.36	-
Brucella	-	25.67	-
MRSA	-	26.41	-
CT	-	25.71	-
TOXO	-	25.79	-
HBV-A	+	93.56	+
HBV-B	+	96.56	+
HBV-C	+	94.34	+
HBV-C(V)	+	96.02	+
HBV-D	+	94.87	+
HBV-E	+	95.67	+
HBV-F	+	95.02	+
HBV-G	+	95.05	+
HBV-H	+	95.36	+

For further analytical specificity testing, HBV strains with known sequence differences in the pre-core region of the HBV genome (HBV Pre-Core Mutant Panel, Teragenix, Florida, USA) were used. The panel contain HBV genotypes A, B, C, C(V), D, E, F, G and H. All 9 pre-core mutant strains of this panel could be detected using the prototype device (Table 4.14).

4.4.4 Linear range

Peter *et al*. (2000) state that PCR will typically be first exponential, then will enter a quasi-linear phase, and finally reach a plateau (Figure 4.20) and end-point PCR product copy number, regardless of the starting copy number, is limited within a copy number range. "A number of factors have been presumed to contribute to this plateau: (1) utilization of substrates (dNTPs or primers); (2) thermal inactivation and limiting concentration of DNA polymerase; (3) inhibition of enzyme activity by increasing pyrophosphate concentration; (4) reannealing of specific product at concentrations above 10^{-8} M; (5) reduction in the denaturation efficiency per cycle" (Peter *et al*., 2000).

Figure 4. 20 Phases of PCR
(http://slideplayer.com/slide/5935537/)
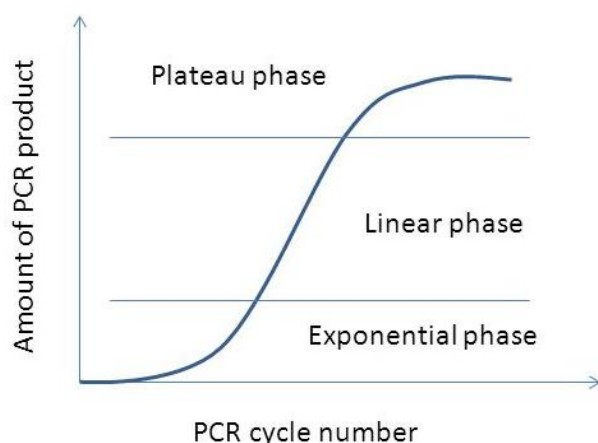
In PCR, end-point PCR product copy number, regardless of the starting copy number, is limited within a copy number range. Thus, end-point analyses such as agarose gel electrophoresis are not quantitative for not giving reliable information about the starting copy number. In the developed microparticle based method, analysis is performed after PCR; so, this method is also an end-point analysis. However, the fluorescence signal reading is the sum of the fluorophore molecules released with the exo-nuclease activity of *Taq* DNA polymerase in each cycle of PCR. Therefore, this method gives information about the starting copy number. But, since end-point PCR product copy number is limited within a copy number range range, huge differences in starting copy numbers do not lead to huge differences in fluorescence intensity readings. The correlation is investigated by plotting fluorescence intensity-versus- $\log_{10}$ of target DNA graph using a dilution series of Artus-Qiagen HBV quantitation standard of $\log_{10}$ concentrations ranging from 2.75 to 8.75 copy/ml (data given in Appendix B, Table B.5). Each dilution was tested in replicates (n = 8). The linear range was determined to cover $\log_{10}$ concentrations from 2.09 copy/ml (limit of detection) to at least 8.75 copy/ml (Figure 4.21). Within this range, the relationship between $\log_{10}$ of target DNA and fluorescence intensity readings is linear. Linear regression analysis comparing the fluorescence intensity-versus- $\log_{10}$ of target DNA was as follows:

$$\text{Fluorescence intensity} = 25.385 \text{ x } (\log_{10} \text{ concentration}) - 24.804 \quad (4.5)$$
$$\text{with a correlation coefficient } (R^2) \text{ of } 0.9928.$$

This means that, for samples with starting $\log_{10}$ concentrations from 2.09 copy/ml to 8.75 copy/ml, the assay may produce quantitative results. The samples having starting $\log_{10}$ concentrations above this range must first be diluted and then be analysed for getting accurate quantitative results.
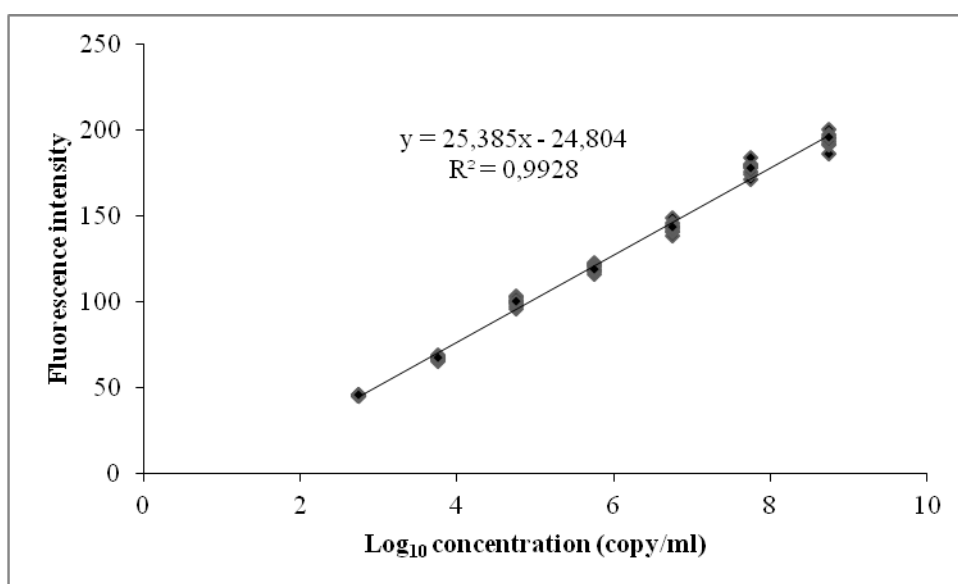
Figure 4. 21 Linear range

4.4.5 Precision

The precision data allow determination of the total variance of the assay. The total variance consists of the intra-assay variability (variability of multiple results of samples of the same concentration within one experiment), the inter-assay variability (variability of multiple results of the assay generated on different days by different operators within one laboratory) and the inter-batch variability (variability of multiple results of the assay using various batches), and inter-brand variability (variability of multiple results of the assay using various PCR tube brands). The data obtained (given in Appendix B, Table B.6) were used to determine the mean, standard deviation, and the coefficient of variation.

Precision data were collected using Artus-Qiagen Quantitation Standard of the lowest concentration (log_{10} concentration of 4.75 copy/ml). Testing was performed with 8 replicates for each variability assay (a total of 32 replicates). The precision data were calculated on basis of fluorescence intensity readings (Table 4.15).

56

Table 4. 15 Precision data on basis of fluorescence readings

	Replicates	Standard Deviation	Mean	Coefficient of variation (%)
Intra-assay variability	8	3.61	95.41	3.79
Inter-assay variability	8	3.57	95.30	3.74
Inter-batch variability	8	3.83	95.51	4.01
Inter-brand variability	8	3.65	95.42	3.82
Total variance	32	3.49	95.41	3.65

In addition, precision data for quantitative results in $\log_{10}$ concentrations (copy/ml) were determined converting fluorescence readings into $\log_{10}$ concentrations by using linear regression analysis (Figure 4.21). The precision data on basis of $\log_{10}$ concentrations is given in Table 4.16. Based on these results (Table 4.15 and Table 4.16), the overall statistical spread of any given sample with the mentioned concentration is 3.65% (fluorescence readings) or 2.90% ($\log_{10}$ concentration).

Table 4. 16 Precision of data on basis of the $\log_{10}$ concentrations

	Replicates	Standard Deviation	Mean	Coefficient of variation (%)
Intra-assay variability	8	0.14	4.74	3.01
Inter-assay variability	8	0.14	4.73	2.97
Inter-batch variability	8	0.15	4.74	3.19
Inter-brand variability	8	0.14	4.74	3.03
Total variance	32	0.14	4.74	2.90

4.4.6 Robustness

The verification of the robustness allows the determination of the total failure rate of the assay. To verify the robustness, 105 HBV negative samples were spiked with Artus-Qiagen Quantitation Standard to give a final $\log_{10}$ concentrations of 2.6 copy/ml in the elution volume which is approximately 3 times the limit of detection value determined by analytical sensitivity study. For all HBV samples the failure rate was 0% (data given in Appendix B, Table B.7). Inhibitions were not observed. Thus, the robustness of the assay is ≥99%.

4.4.7 Diagnostic evaluation

To compare the quantitation values of prototype device with Roche COBAS TaqMan HBV assay; 105 HBV (-) and 187 HBV (+) samples "tested previously with Roche COBAS TaqMan HBV assay" were examined with prototype device (data given in Appendix B, Table B.8).

In comparison to the results collected with the Roche COBAS TaqMan HBV Assay (a reference assay used for validation in the majority of commercial assays), a diagnostic sensitivity of the prototype device of 97.9% and a diagnostic specificity of 100% was determined for the totality of all samples. These results are given in Table 4.17.

Table 4. 17 Results of the comperative validation study

		Roche COBAS TaqMan HBV assay		
		+	-	Total
Prototype Device	+	183	0	183
	-	4	105	109
	Total	187	105	

The correlation of the quantitative results of both test systems was analyzed by linear regression. The results of both assays are shown in comparison in Figure 4.22. The fitted regression line was given by the equation:

$$\log_{10} (\text{Roche copies/ml}) = 0.9953 \times \log_{10} (\text{Prototype copies/ml}) + 0.0464 \quad (4.6)$$

with a correlation coefficient (R^2) of 0.9971.

Pearson's correlation coefficient was used to assess the strength of the linear association between the log-transformed values of Prototype and Roche assays; correlation coefficient (R^2) is calculated as 0.9971.

To compare results obtained by two different methods, the fitted regression lines were compared with the line of equality by testing the two-tailed hypothesis of slope = 1 and intercept = 0. The intercept of the fitted regression line did not differ significantly from "0" (intercept = 0.0464) and the slope of the fitted regression line did not differ significantly from "1" (slope = 0.9953).
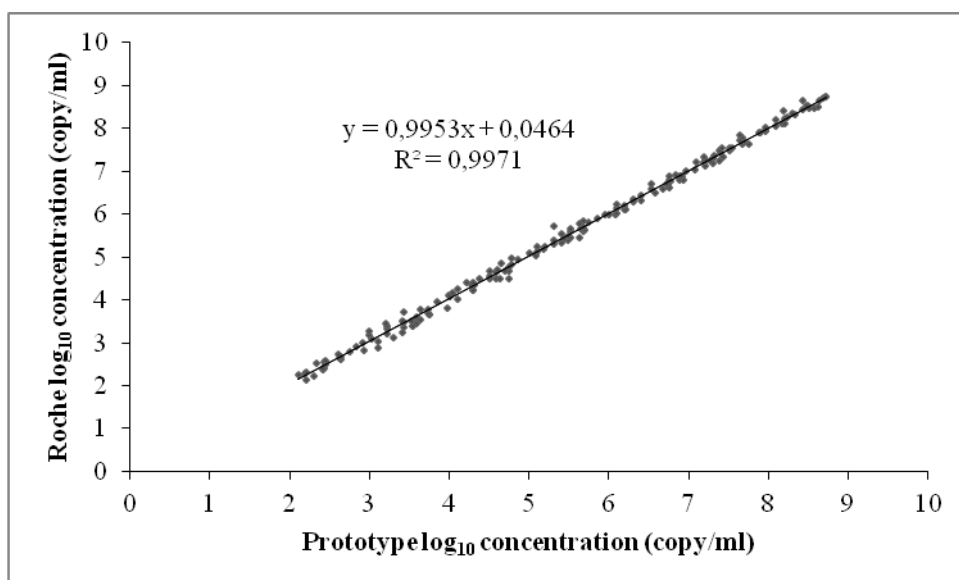
Figure 4. 22 Correlation plot of log$_{10}$ HBV DNA values (Roche/Prototype)

CHAPTER 5

CONCLUSIONS

Quantitative PCR is a fast and reliable method; however, the price of quantitative PCR devices are relatively expensive; the prices range between 25,000 € and 100,000 €. Equipment using the combination of PCR and agarose gel electrophoresis methods are lower in price (about 25,000 €) but have several disadvantages such as long analysis periods (4-5 hours), contamination risk, false positivity risk, and usage of carcinogenic chemicals (ethidium bromide). In this study, a nucleic acid based in-vitro diagnostic device operating with a novel microparticle based method is designed, manufactured and validated. In this microparticle based method, PCR is performed with the presence of microparticles and oligonucleotide probes. Oligonucleotide probes that are unused in PCR adsorb onto the microparticules; however, fluorophore molecules released with the exo-nuclease activity of *Taq.* DNA polymerase does not adsorb onto microparticles. By this way, background fluorescence is reduced and the need for sensitive sensors for detecting the fluorescence difference disappears.

A prototype device including a LED (light emitting diode) light source, two filter sliders, two excitation band-pass filters (490 nm and 650 nm wavelength), a 24 sample carousel, two emission band-pass filters (520 nm and 670 nm wavelength), and a CCD (charge-coupled device) camera was designed and manufactured with a cost of 500 €. Along with cost reduction, the invented method introduces some advantages. First of all, the device is light; the prototype device is about 2.6 kg. Secondly, analysis duration is reduced since agarose gel electrophoresis is not practiced. Thirdly, cross-over contamination is prevented since PCR tube caps are not opened. Moreover, false positivity problem which

may occur because of false priming is avoided with the usage of oligonucleotide probes. Finally, carcinogenic chemical ethidium bromide is not used since agarose gel electrophoresis is not practiced and oligonucleotide probes are used for detection purposes.

Microparticle batch equilibrium analysis was performed by using the measured liquid and solid phase solute (probe) equilibrium concentrations. The equilibrium data obtained was described by linear type isotherm where linear equilibrium constant (K) is calculated as 0.0532 ($pmol_{solid}$ / μg particle) / ($pmol_{liquid}$ /μl). Calculated linear equilibrium constant may be useful for estimating microparticle concentration for different PCR total volumes.

Using DNA eluates from 105 HBV negative-diagnosed and 187 HBV positive-diagnosed samples, prototype device validation study including cutoff score, analytical sensitivity, analytical specificity, linear range, precision, robustness, diagnostic sensitivity, and diagnostic specificity was conducted. The cutoff score for prototype diagnostic device for classifying cases as positive and negative is determined to be 27.45 (fluorescence intensity units). The 95% limit of detection log_{10} concentration is calculated as 2.09 copy/ml. The linear range was determined to cover log_{10} concentrations from 2.09 copy/ml to at least 8.75 copy/ml. The overall statistical spread of any given sample with log_{10} concentration of 4.75 copy/ml is calculated as 3.65% (fluorescence readings) or 2.90% (log_{10} concentration). In comparison to the results collected with reference assay, a diagnostic sensitivity of the prototype device of 97.9% and a diagnostic specificity of 100% was determined for the totality of all samples. These findings suggest that low-cost prototype device combines high sensitivity, specificity, reproducibility and accuracy for HBV DNA quantitation in a high linear range.

In this study, a nucleic acid based in-vitro diagnostic device operating with a novel microparticle based method is designed, manufactured and validated for HBV diagnosis. Developed nucleic acid based in-vitro diagnostic device may also be used for diagnosis of microbiological and genetic diseases, genetically modified organisms, and biological weapons. Since the device will be an open

platform, novel R&D projects can be initiated on the development of new diagnostic kits working on this device. In the development of new diagnostic kits, fluorophores with high fluorescence quantum yields may be used in order to increase efficiencies of the assays.

There is also further improvement potential over time compared to the existing solution. First of all, PCR cycle number optimization study may be conducted in order to gain results from exponential and quasi-linear phases affording the risk of increase in sensor costs. Secondly, the device is already light but may be produced to be lighter. Furthermore, the device may gather fluorescence intensity readings through mobile phone cameras introducing total portability eliminating the need for electricity. Moreover, the device may use telecommunication technologies to send analysis reports to related parties by e-mail or cloud technologies. By the use of micro electro-mechanical systems (MEMS), the device may be upgraded to perform nucleic acid extraction, as well. By this way, the device may be used for food inspection at the customs gates and for detection and characterization of biological weapons in the case of biological warfare. Finally, point-of-care testing may be possible with these improvements over time.

REFERENCES

Abdul Khaliq R., Sonawane P.J., Sasi B.K., Sahu B.S., Pradeep T., Das S.K., (2010), Enhancement in the efficiency of polymerase chain reaction by TiO_2 nanoparticles: crucial role of enhanced thermal conductivity, Nanotechnology 21 2010 255704

Ayaz, Y., Ayaz, N. D., Erol, I. (2006). Detection of species in meat and meat products using enzyme-linked immunosorbent assay. Journal of Muscle Foods, 17(2), 214 220.

Bailey J., Ollis E. (1986). In: Biochemical Engineering fundamentals 2nd ed, pp: 745-749.

Berger, A., Preiser, W., Doerr, H.W. (2001). The role of viral load determination for the management of human immunodeficiency virus, hepatitis B virus and hepatitis C virus infection. J. Clin. Virol. 20, 23–30.

Bruno J.G. (1997). In vitro selection of DNA to chloroaromatics using magnetic microbead-based affinity separation and fluorescence detection. Biochem. Biophys. Res. Comm. 234, 117–120.

Bustin S.A., Benes V., Garson J.A., Hellemans J., Huggett J., Kubista M., Mueller R., Nolan T., Pfaffl M.W., Shipley G.L., Vandesompele J. (2009). The MIQE guidelines: minimum information for publication of quantitative real-time PCR experiments, Clin. Chem. 55 4 2009 Apr 1 611–622

Cetus Corporation (Emeryville, CA). 1987. United States Patent. 4,683,202

Cetus Corporation (Emeryville, CA). 1989. United States Patent. 4,889,818

CLSI (Clinical and Laboratory Standards Institute). (2012). Evaluation of detection Capability for Clinical Laboratory Measurement Procedures; Approved Guideline, second ed. CLSI document EP17eA2.

Conrad, R., Giver, L., Tian, Y., and Ellington, A. (1996). In vitro selection of nucleic acid aptamers that bind proteins. Methods Enzymology 267: 336-367.

Coren A. Milbury, Qun Zhong, Jesse Lin, Miguel Williams, Jeff Olson, Darren R. Link, Brian Hutchison. (2014). Determining lower limits of detection of digital PCR assays for cancer-related gene mutations. Biomolecular Detection and Quantification 1 2014 8–22

Danielle Alves Gomes Zauli, Carla Lisandre Paula de Menezes, Cristiane Lommez de Oliveira, Elvis Cristian Cueva Mateo, Alessandro Clayton de Souza Ferreira. (2016). In-house quantitative real-time PCR for the diagnosis of hepatitis B virus and hepatitis C virus infections, Brazilian journal of microbiology 47 2016 987–992

Devine KG, Reese CB. (1986). Highly reactive condensing agents for the synthesis of oligonucleotides by the phosphotriester approach. Tetrahedron Lett. 27(45), 5529-32.

Dötsch J, Schoof E, Wolfgang Rascher W. (2005). Quantitative TaqMan real-time PCR, diagnostic and scientific applications. In: Walker JM, Rapley R, editors. Medical biomethods handbook. Totowa, NJ: Humana Press; 2005, p. 305–13.

Dramane Kania, Laure Ottomani, Nicolas Meda, Marianne Peries, Pierre Dujols, Karine Bolloré, Wendy Rénier, Johannes Viljoen, Jacques Ducos, Philippe Van de Perre, Edouard Tuaillon. (2014). Performance of two real-time PCR assays for hepatitis B virus DNA detection and quantitation, Journal of Virological Methods 201 2014 24–30

Eastman Kodak Company (Rochester, NY). 1990. United States Patent. 4,902,624

Ellison S.L.R., Fearn T. (2005). Characterising the performance of qualitative analytical methods: Statistics and terminology, Trends in Analytical Chemistry, Vol. 24, No. 6, 2005

EP17-A, C.L.S.I. (2004). Protocols for Determination of Limits of Detection and Limits of Quantitation; Approved Guideline, CLSI, Wayne PA, 2004.

Erlich, H.A. (1989) PCR Technology: Principles and Applications for DNA Amplification, pp. 1-7, Stockton Press, New York, NY.

Finney, D. J., Ed. (1952). Probit Analysis. Cambridge, England, Cambridge University Press.

Frahm E, Obst U. (2003). Application of the fluorogenic probe technique (TaqMan PCR) to the detection of Enterococcus spp. and Escherichia coli in water samples. J Microbiol Methods. 2003 Jan;52(1):123-31.

Galvão LMC, Lages-Silva E. (2008). Randomly amplified polymorphic DNA (RAPD) - A useful tool for genomic characterization of different organisms. In: Walker JM, Rapley R, editors. Molecular biomethods handbook. Totowa, NJ. Humana Press; 2008, p. 133–47.

Garson J.A., Grant P.R., Ayliffe U., Ferns R.B., Tedder R.S. (2005). Real-time PCR quantitation of hepatitis B virus DNA using automated sample preparation and murine cytomegalovirus internal control, Journal of Virological Methods 126 2005 207–213

Gaudet M, Fara AG, Beritognolo I, Sabatti M. (2009). Allele-specific PCR in SNP genotyping. In: Komar AA, editor. Single nucleotide polymorphisms, methods in molecular biology 578. New York; Humana Press; 2009, p. 415–24.

Gibson, U.E., Heid, C.A., Williams, P.M. (1996). A novel method for real time quantitative RT-PCR. Genome Res. 6, 995–1001.

Glavac D, Dean M. (1993). Optimization of the single-strand conformation polymorphism (SSCP) technique for detection of point mutations. Hum Mutat 1993;2:404 –14.

Gold, L. (1995). Oligonucleotides as research, diagnostic, and therapeutic agents. J. Biol. Chem. 270: 13581-4.

Graham, C., and Hill, A. (2001) in Methods in Molecular Biology: DNA Sequencing Protocols (Vol 167) pp. 1-244, Humana Press Inc., Totowa, NJ.

Guichoux E, Lagache L, Wagner S, Chaumeil P, Léger P, Lepais O, (2011). Current trends in microsatellite genotyping. Mol Ecol Resour 2011;11:591– 611.

Heid, C.A., Stevens, J., Livak, K.J., Williams, P.M., (1996). Real time quantitative PCR. Genome Res. 6, 986–994.

Higuchi, R., Fockler, C., Dollinger, G., Watson, R. (1993). Kinetic PCR: real time monitoring of DNA amplification reactions. Biotechnology 11, 1026–1030.

Higuchi; Russell Gene (Alameda, Alameda County, CA). 2004. United States Patent. 6,814,934

Hoffman-La Roche Inc. (Nutley, NJ). 1993. United States Patent. 5,210,015

Hongna Liu, Song Li, Zhifei Wang, Meiju Ji, Libo Nie, Nongyue Hea, (2007), High-throughput SNP genotyping based on solid-phase PCR on magnetic nanoparticles with dual-color hybridization, Journal of Biotechnology 131 2007 217–222

Hongyan Su, Xiaochun Meng, Qiuping Guo, Yongjun Tan, Qingyun Cai, Hongtao Qin, Xiangxian Menn, (2014), Label-free DNAsensor with PCR-like sensitivity based on background reduction and target-triggered polymerization amplification, Biosensors and Bioelectronics 52 2014 417–421

Hou, B., Meng, X., Zhang, L., Guo, J., Li, S., & Jin, H. (2014). Development of a sensitive and specific multiplex PCR method for the simultaneous detection of chicken, duck and goose DNA in meat products. Meat Science, 101C, 90–94.

Hua Kuanga, Shuge Zhaoa, Wei Chena, Wei Maa, Qianqian Yonga, Liguang Xua, Libing Wanga, Chuanlai Xua, (2011), Rapid DNA detection by interface PCR on nanoparticles, Biosensors and Bioelectronics 26 2011 2495–2499

Huang H. Li, J., An J. Lv, H., Zhang X., Zhang Z., (2005), Nanoparticle PCR: nanogold-assisted PCR with enhanced specificity, Angew. Chem. Int. Ed. 44 2005 5100–5103

Jayasena, S. (1999). Aptamers: An Emerging Class of Molecules That Rival Antibodies in Diagnostics. Clinical Chemistry 45: 1628-1650.

Jinxiu Shi, Basangzhuoma, Zhigang Xing, Yangla, Chaoying Cui. (2012). Establishment of rapid and specific real-time PCR assays for the detection of hepatitis B viral genotype in Tibet, Journal of Virological Methods 183 2012 75–79

John T. Corthell. (2014). Agarose Gel Electrophoresis. Basic Molecular Protocols in Neuroscience: Tips, Tricks, and Pitfalls, pp.21-25

Karlsson, A. O., Holmlund, G. (2007). Identification of mammal species using species-specific DNA pyrosequencing. Forensic Science International, 173(1), 16 20.

Kavita S. Lole, Vidya A. Arankalle. (2006). Quantitation of hepatitis B virus DNA by real-time PCR using internal amplification control and dual TaqMan MGB probes, Journal of Virological Methods 135 2006 83–90

Kleparník K, Bocek P. (2007). DNA diagnostics by capillary electrophoresis. Chem Rev 2007;107:5279 –317.

Laude A., Valot S., Desoubeaux G., Argy N., Nourrisson C., Pomares C., Machouart M., Le Govic Y., Dalle F., Botterel F., Bourgeois N., Cateau E., Leterrier M., Le Pape P., Morio F. (2016). Is real-time PCR-based diagnosis similar in performance to routine parasitological examination for the identification of Giardia intestinalis, Cryptosporidium parvum/Cryptosporidium hominis and Entamoeba histolytica from stool samples? Evaluation of a new commercial multiplex PCR assay and literature review. Clin Microbiol Infect. 2016 Feb;22(2):190.e1-190.e8.

Letsinger RL, Mahadevan V. (1965). Oligonucleotide synthesis on a polymer support. J. Am. Chem. Soc. 87(15), 3526-7.

Liang G., Ma C., Zhu Y., Li S., Shao Y., Wang Y., (2010), Enhanced specificity ofmultiplex polymerase chain reaction via CdTe quantum dots, Nanoscale Res.Lett. 6 2010 51,

Liesbet Deprez, Philippe Corbisier, Anne-Marie Kortekaas, Stéphane Mazoua, Roxana Beaz Hidalgo, Stefanie Trapmann, Hendrik Emons. (2016). Validation of a digital PCR method for quantification of DNA copy number concentrations by using a certified reference material, Biomolecular Detection and Quantification 9 2016 29–39

Locarnini, S., Birch, C. (1999). Antiviral chemotherapy for chronic hepatitis B infection: lessons learned from treating HIV-infected patients. J. Hepatol. 30, 536–550.

Lorena Manzanares-Palenzuela C., Isabel Mafraa, Joana Costa, Fátima Barroso M.,Noemí de-los-Santos-Álvarezd, Cristina Delerue-Matos, Beatriz P.P. Oliveira M., Jesus Lobo-Casta˜nón M., Beatriz López-Ruiz, (2016), Electrochemical magnetoassay coupled to PCR as a quantitativeapproach to detect the soybean transgenic event GTS40-3-2 in foods, Sensors and Actuators B 222 2016 1050–1057

Lynne M. Sloan. (2007). Real-Time PCR in Clinical Microbiology: Verification, Validation, and Contamination Control, Clinical Microbiology Newsletter Vol. 29, No. 12

Mafra, I., Ferreira, I. M. P. L. V. O., & Oliveira, M. B. P. P. (2008). Food authentication by PCR-based methods. European Food Research and Technology, 227(3), 649 665.

Mahsa Osmani Bojd, Hossein Kamaladini, Fatemeh Haddadi, Akbar Vaseghi, (2017), Thiolated AuNP probes and multiplex PCR for molecular detection of Staphylococcus epidermidis, Molecular and Cellular Probes 34 2017 30e36

Manuela da Silva Solcà, Carlos Eduardo Sampaio Guedes, Eliane Gomes Nascimento, Geraldo Gileno de Sá Oliveira, Washington Luis Conrado dos Santos, Deborah Bittencourt Mothé Fraga, Patrícia Sampaio Tavares Veras. (2012). Qualitative and quantitative polymerase chain reaction (PCR) for detection of Leishmania in spleen samples from naturally infected dogs. Veterinary Parasitology 184 2012 133–140

Marc I. Glazer, Jacqueline A. Fidanza, Glenn H. McGall, Mark O. Trulson, Jonathan E. Forman, Curtis W. Frank. (2007). Kinetics of Oligonucleotide Hybridization to DNA Probe Arrays on High-Capacity Porous Silica. Biophys J. 2007 Sep 1; 93(5): 1661–1676.

Matteucci MD, Caruthers MH. (1981). Synthesis of deoxyoligonucleotides on a polymer support. J. Am. Chem. Soc. 103: 3185-3191.

Michael Famulok, Andreas Jenne. (1998). Oligonucleotide libraries - variatio delectat. Current Opinion in Chemical Biology Volume 2, Issue 3, June 1998, Pages 320-327

Ming-Liang He, Jun Wu, Ying Chen, Marie C. Lin, George K.K. Lau, and Hsiang-fu Kung. (2002). A new and sensitive method for the quantification of HBV cccDNA by real-time PCR, Biochemical and Biophysical Research Communications 295 2002 1102–1107

Morinha F, Cabral JA, Bastos E. (2012). Molecular sexing of birds: A comparative review of polymerase chain reaction (PCR)-based methods. Theriogenology. 2012 Sep 1;78(4):703-14.

Mueller UG, Wolfenbarger LL. (1999). AFLP genotyping and fingerprinting. Trends Ecol Evol 1999;14:389 –94.

Navarro E, Serrano-Heras G, Castaño MJ, Solera J. (2015). Real-time PCR detection chemistry. Clin Chim Acta. 2015 Jan 15;439:231-50. doi: 10.1016/j.cca.2014.10.017. Epub 2014 Oct 22

Nick Saundersa, Maria Zambona, Ian Sharpa, Ruhi Siddiquia, Alison Berminghama, Joanna Ellis, Barry Vipond, Andrew Sails, Jacob Moran-Gilad, Peter Marsh, Malcolm Guiver. (2013). Guidance on the development and validation of diagnostic tests that depend on nucleic acid amplification and detection, Journal of Clinical Virology 56 2013 260– 270

Oster CG, Kim N, Grode L, Barbu-Tudoran L, Schaper AK, Kaufmann SH, Kissel T. (2005). Cationic microparticles consisting of poly(lactide-co-glycolide) and polyethylenimine as carriers systems for parental DNA vaccination. J Control Release. 2005 May 18;104(2):359-77. Epub 2005 Apr 15.

Paraskevis D, Haida C, Tassopoulos N, Raptopoulou M, Tsantoulas D, Papachristou H, Sypsa V, Hatzakis A. (2002). Development and assessment of a novel real-time PCR assay for quantitation of HBV DNA. J Virol Methods. 2002 May 16;103(2):201-12.

Perrillo, R.P., Schiff, E.R., Davis, G.L., Bodenheimer, H.C. Jr., Lindsay, K., Payne, J., Dienstag, J.L., O'Brien, C., Tamburro, C., Jacobson, I.M., *et al.* (1990). A randomized, controlled trial of interferon alfa-2b alone and after prednisone withdrawal for the treatment of chronic hepatitis B. N. Engl. J. Med. 323, 295–301.

Peter Kainz, (2000), The PCR plateau phase - towards an understanding of its limitations, Biochimica et Biophysica Acta 1494 2000 23-27

Petersen, J., Poulsen, L., Petronis, S., Birgens, H., Dufva, M., (2008), Use of a multithermal washer for DNA microarrays simplifies probe design and gives robust genotyping assays. Nucleic Acids Res. 36, e10.

Pfleiderer, W., Matysiak, S., Bergmann, F., and Schnell, R. (1996). Recent progress in oligonucleotide synthesis. Acta Biochimica Polonica 43: 37-44.

Pollard, J., Bell, S.D., Ellington, A.D., (2000). Generation and use of combinatorial libraries. In: Ausubel, G., Brent, F.M., Kingston, R., Moore, R.E., Seidman, D.D., Smith, J.G., Struhl, K. (Eds.), Current Protocols in Molecular Biology, vol. 4. Greene Publishing Associates, JohnWiley Liss&Sons, Inc., New York, NY, USA, pp. 24.21.21–24.25.34.

Pourzand C, Cerutti P. (1993). Genotypic mutation analysis by RFLP/PCR. Mutat Res 1993;288:113–21

Priyanka Kambli, Varsha Kelkar-Mane, (2016), Nanosized Fe3O4an efficient PCR yield enhancer—Comparative studywith Au, Ag nanoparticles, Colloids and Surfaces B: Biointerfaces 141 2016 546–55

Pryor RJ, Wittwer CT. (2006). Real-time polymerase chain reaction and melting curve analysis. Methods Mol Biol 2006;336:19–32.

Qiuying Huang, Qingge Li. (2009). Characterization of the 5' to 3' nuclease activity of *Thermus aquaticus* DNA Polymerase. Molecular and Cellular Probes 23(3-4):188-94

Reed GH, Kent JO, Wittwer CT. (2007). High-resolution DNA melting analysis for simple and efficient molecular diagnostics. Pharmacogenomics 2007;8:597–608.

Robert J. Tibbetts, Henry Ford. (2015). Verification and Validation of Tests Used in the Clinical Microbiology Laboratory, Clinical Microbiology Newsletter Vol. 37, No. 19 October 1, 2015

Sang Hyun Hwang, Dong-EunKim, Ji-HyunIm, Su-JinKang, Do-HoonLee, Sang JunSon, (2016), Rapid visual identification of PCR amplified nucleic acids by centrifugal gel separation: Potential use for molecular point-of-care tests, Biosensors and Bioelectronics 79 2016 829–834

Sang-Hyun Hwang, Dong-EunKim, Ji-HyunIm, Su-JinKang, Do-HoonLee, Sang JunSon. (2016). Rapid visualidentification of PCR amplified nucleic acids by centrifugal gelseparation: Potential use for molecular point-of-care tests. Biosensors and Bioelectronics 79 2016 829–834

Sena Izmirli, Deniz Gozde Celik, Pelin Yuksel, Suat Saribas, Mustafa Aslan, Sevgi Ergin, Hrisi Bahar, Sümeyye Sen, Bulent Cakal, Ali Oner, Bekir Kocazeybek. (2012). The detection of occult HBV infection in patients with HBsAg negative pattern by real-time PCR method, Transfusion and Apheresis Science 47 2012 283–287

Seungwon Junga, Jungmin Kima, Junsun Kima, Sang Hwa Yang, Sang Kyung Kim, (2017), Extensible multiplex real-time PCR for rapid bacterial identification with carbon nanotube composite microparticles, Biosensors and Bioelectronics 94 2017 256–262

Shantanu Prakash, Amita Jain , Bhawana Jain. (2016). Development of novel triplex single-step real-time PCR assay for detection of Hepatitis Virus B and C simultaneously, Virology 492 2016 101–107

Singh G. (2006). Determination of Cutoff Score for a Diagnostic Test. The Internet Journal of Laboratory Medicine. 2006 Volume 2 Number 1.

Sumedha D. Jayasena (1999). Aptamers: An Emerging Class of Molecules That Rival Antibodies in Diagnostics. Clinical Chemistry 45:9 1628–1650.

Teletchea, F., Bernillon, J., Duffraisse, M., Laudet, V., & Hanni, C. (2008). Molecular identification of vertebrate species by oligonucleotide microarray in food and forensic samples. Journal of Applied Ecology, 45(3), 967 975.

Tobe, S. S., & Linacre, A. M. T. (2008). A multiplex assay to identify 18 European mammal species from mixtures using the mitochondrial cytochrome b gene. Electrophoresis, 29(2), 340 347.

Toshiaki Higashi, Hiroaki Minegishi, Akinobu Echigo, Yutaka Nagaoka, Takahiro Fukuda,Ron Usami, Toru Maekawa, Tatsuro Hanajiri, (2015), Nanomaterial-assisted PCR based on thermal generation from magnetic nanoparticles under high-frequency AC magnetic fields, Chemical Physics Letters 635 2015 234–240

Tuerk, C., Gold, L., (1990). Systematic evolution of ligands by exponential enrichment: RNA ligands to bacteriophage T4 DNA polymerase. Science 249. 505–510.

Violeta Fajardo, Isabel Gonza´lez, Marı´a Rojas, Teresa Garcı´a and Rosario Martı´n. (2010). A review of current PCR-based methodologies for the authentication of meats from game animal species. Trends in Food Science & Technology 21 2010 408 421

Wan W.W.W., Yeow J.T.W., Van Dyke M.I., (2009), Effect of silver and titaniumdioxide nanoparticles on PCR efficiency, 2009 9th IEEE Conf. Nanotechnol. 2009.

Wang, D., Tian, L., Zhao, Y. (2017). Smoothed empirical likelihood for the Youden index. Computational Statistics and Data Analysis 2017 S0167-9473(17)30059-2

Wei Wang, Hongpin Liang, Yongbin Zeng, Jinpiao Lin, Can Liu, Ling Jiang, Bin Yang , Qishui Ou. (2014). Establishment of a novel two-probe real-time PCR for simultaneously quantification of hepatitis B virus DNA and distinguishing genotype B from non-B genotypes, Clinica Chimica Acta 437 2014 168–174

Wei, C.-W., Cheng, J.-Y., Huang, C.-T., Yen, M.-H., Young, T.-H., (2005), Using a microfluidic device for DNA microarray hybridization in 500 s. Nucleic Acids Res. 33.

Weiss J., Wu H., Farrenkopf B., Schultz T., Song G., Shah S., Siegel J. (2004). Real time TaqMan PCR detection and quantitation of HBV genotypes A–G with the use of an internal quantitation standard, Journal of Clinical Virology 30 2004 86–93

Xiaoteng Luo, Jingjing Xu, John Barford, I-Ming Hsing, (2010), Magnetic particle based electrochemical sensing platform for PCR amplicon detection, Electrochemistry Communications 12 2010 531–534

Yan Liua, Debin Zhua, Yujuan Caoa, Wenge Mab, Ying Yua, Manli Guoa, Xiaobo Xinga, (2017), A novel universal signal amplification probe-based electrochemiluminescence assay for sensitive detection of pathogenic bacteria, Electrochemistry Communications 85 2017 11–14

Youden,W.J., (1950). Index for rating diagnostic tests. Cancer 3, 32–35.

Zarski, J.P., Kuhns, M., Berck, L., Degos, F., Schalm, S.W., Tiollais, P., Brechot, C. (1989). Comparison of a quantitative standardized HBV DNA assay and a classical spot hybridization test in chronic active hepatitis B patients undergoing antiviral therapy. Res. Virol. 140, 2830–2831.

Zhang Z., Shen C., Wang M., Han H., Cao X., (2008), Aqueous suspension of carbonnanotubes enhances the specificity of long PCR, Biotechniques 44 2008 537–545

Zoulim, F., Mimms, L., Floreani, M., Pichoud, C., Chemin, I., Kay, A., Vivitski, L., Trepo, C. (1992). New assays for quantitative determination of viral markers in management of chronic hepatitis B virus infection. J. Clin. Microbiol. 30, 1111–1119.

APPENDIX A

CHEMICALS USED IN THE EXPERIMENTS

Table A. 1 The chemicals used and the suppliers for the chemicals

Reagent	Supplier
Ethanol	Merck
Polyacrylic acid MW 1800	Sigma
Glycidyl methacrylate	Sigma
Benzoyl peroxide	Sigma
Ammonia %25	Sigma
Polyvinylpyrollidone K-30	Sigma
Taq DNA polymerase	Sigma
dNTP's set	Sigma
Ethidium bromide	Sigma
Agarose	Sigma
TBE buffer	Sigma
Bromophenol blue	Sigma
100 bp DNA ladder	Sigma

DATA OF FIGURES IN CHAPTER 4

Table B. 1 Data of Figure 4.15

$(C^0_{pro}-C_{pro})/C^0_{pro}$	$C_{particle}$, μg/μl
0.000	0
0.325	5
0.523	10
0.702	15
0.757	20
0.853	25
0.965	**30**
0.965	35
0.967	40

Table B. 2 Data of Figure 4.16

q, pmol probe/μg particle	y, pmol/μl
0.012980	0.135100
0.010468	0.095320
0.009364	0.059540
0.007567	0.048660
0.006824	0.029400
0.006432	0.007040

Table B. 3 Data of cutoff score determination study

Sample Number	Known Qualitative Diagnosis (+/-)	Prototype Fluorescence Intensity
RN001	-	26.51
RN002	-	26.53
RN003	-	26.48
RN004	-	25.59
RN005	-	25.61
RN006	-	25.63
RN007	-	26.55
RN008	-	25.30
RN009	-	26.46
RN010	-	25.33
RN011	-	25.36
RN012	-	26.57
RN013	-	25.44
RN014	-	26.44
RN015	-	25.46
RN016	-	26.59
RN017	-	25.48
RN018	-	26.42
RN019	-	25.50
RN020	-	26.61
RN021	-	25.53
RN022	-	26.40
RN023	-	25.55
RN024	-	26.62
RN025	-	25.32
RN026	-	26.38
RN027	-	25.34
RN028	-	26.64
RN029	-	26.34
RN030	-	25.36
RN031	-	26.36
RN032	-	25.38
RN033	-	26.66

Table B.3 (continued)

RN034	-	26.32
RN035	-	25.40
RN036	-	26.30
RN037	-	26.68
RN038	-	25.42
RN039	-	26.28
RN040	-	24.67
RN041	-	26.70
RN042	-	26.01
RN043	-	26.26
RN044	-	26.02
RN045	-	27.12
RN046	-	26.72
RN047	-	26.24
RN048	-	26.03
RN049	-	26.74
RN050	-	25.39
RN051	-	25.42
RN052	-	26.78
RN053	-	25.45
RN054	-	25.28
RN055	-	26.04
RN056	-	25.26
RN057	-	26.82
RN058	-	25.99
RN059	-	25.98
RN060	-	26.22
RN061	-	25.97
RN062	-	26.21
RN063	-	26.05
RN064	-	26.86
RN065	-	25.30
RN066	-	25.96
RN067	-	26.90
RN068	-	25.94
RN069	-	26.00

Table B.3 (continued)

RN070	-	26.10
RN071	-	26.93
RN072	-	25.63
RN073	-	26.06
RN074	-	24.83
RN075	-	26.97
RN076	-	26.18
RN077	-	25.65
RN078	-	25.93
RN079	-	25.67
RN080	-	26.07
RN081	-	25.71
RN082	-	25.75
RN083	-	27.32
RN084	-	25.92
RN085	-	25.79
RN086	-	26.08
RN087	-	25.83
RN088	-	26.16
RN089	-	25.91
RN090	-	25.84
RN091	-	26.14
RN092	-	25.77
RN093	-	25.67
RN094	-	26.09
RN095	-	25.86
RN096	-	25.87
RN097	-	25.89
RN098	-	26.12
RN099	-	25.49
RN100	-	25.90
RN101	-	25.53
RN102	-	25.60
RN103	-	25.92
RN104	-	26.11
dH_2O	-	25.56

Table B.3 (continued)

RP001	+	25.42
RP002	+	27.45
RP003	+	26.69
RP004	+	26.18
RP005	+	25.93
RP006	+	31.25
RP007	+	33.78
RP008	+	28.72
RP009	+	30.74
RP010	+	31.00
RP011	+	36.57
RP012	+	37.08
RP013	+	36.57
RP014	+	37.33
RP015	+	34.29
RP016	+	37.08
RP017	+	37.33
RP018	+	42.40
RP019	+	41.64
RP020	+	42.14
RP021	+	41.38
RP022	+	45.18
RP023	+	49.74
RP024	+	54.05
RP025	+	46.96
RP026	+	49.24
RP027	+	54.05
RP028	+	52.02
RP029	+	59.12
RP030	+	51.26
RP031	+	57.09
RP032	+	61.90
RP033	+	51.26
RP034	+	57.09
RP035	+	62.41
RP036	+	64.94

Table B.3 (continued)

RP037	+	56.84
RP038	+	65.20
RP039	+	56.58
RP040	+	66.46
RP041	+	62.41
RP042	+	64.69
RP043	+	61.65
RP044	+	67.48
RP045	+	66.21
RP046	+	66.46
RP047	+	70.26
RP048	+	70.52
RP049	+	70.01
RP050	+	62.41
RP051	+	67.48
RP052	+	70.01
RP053	+	76.09
RP054	+	72.80
RP055	+	79.39
RP056	+	76.85
RP057	+	76.60
RP058	+	77.61
RP059	+	84.45
RP060	+	84.45
RP061	+	79.39
RP062	+	83.95
RP063	+	84.71
RP064	+	82.17
RP065	+	84.45
RP066	+	86.48
RP067	+	91.55
RP068	+	92.81
RP069	+	95.60
RP070	+	89.77
RP071	+	89.77
RP072	+	91.55

Table B.3 (continued)

RP073	+	95.60
RP074	+	94.59
RP075	+	89.77
RP076	+	92.05
RP077	+	95.60
RP078	+	96.61
RP079	+	93.32
RP080	+	98.39
RP081	+	96.61
RP082	+	104.21
RP083	+	102.19
RP084	+	104.72
RP085	+	106.75
RP086	+	104.72
RP087	+	107.00
RP088	+	110.04
RP089	+	112.57
RP090	+	109.79
RP091	+	114.35
RP092	+	113.08
RP093	+	118.15
RP094	+	115.36
RP095	+	114.35
RP096	+	112.57
RP097	+	115.36
RP098	+	119.41
RP099	+	119.92
RP100	+	115.36
RP101	+	118.40
RP102	+	119.41
RP103	+	109.79
RP104	+	118.15
RP105	+	120.93
RP106	+	119.41
RP107	+	123.97
RP108	+	126.25

Table B.3 (continued)

RP109	+	129.55
RP110	+	127.52
RP111	+	130.05
RP112	+	132.33
RP113	+	132.84
RP114	+	129.80
RP115	+	132.33
RP116	+	129.80
RP117	+	135.12
RP118	+	137.65
RP119	+	135.12
RP120	+	137.65
RP121	+	142.21
RP122	+	144.75
RP123	+	141.20
RP124	+	146.77
RP125	+	146.27
RP126	+	145.76
RP127	+	141.20
RP128	+	147.03
RP129	+	149.81
RP130	+	151.33
RP131	+	146.77
RP132	+	146.77
RP133	+	150.83
RP134	+	149.81
RP135	+	150.32
RP136	+	148.80
RP137	+	152.09
RP138	+	154.88
RP139	+	158.17
RP140	+	160.45
RP141	+	155.39
RP142	+	157.92
RP143	+	159.95
RP144	+	162.48

Table B.3 (continued)

RP145	+	158.17
RP146	+	160.45
RP147	+	157.92
RP148	+	163.75
RP149	+	161.21
RP150	+	163.24
RP151	+	162.48
RP152	+	166.03
RP153	+	165.77
RP154	+	163.49
RP155	+	166.53
RP156	+	170.08
RP157	+	172.11
RP158	+	170.08
RP159	+	170.59
RP160	+	169.32
RP161	+	170.08
RP162	+	169.32
RP163	+	175.65
RP164	+	175.15
RP165	+	177.17
RP166	+	177.43
RP167	+	177.43
RP168	+	180.72
RP169	+	182.75
RP170	+	183.51
RP171	+	180.72
RP172	+	183.51
RP173	+	184.27
RP174	+	186.55
RP175	+	186.04
RP176	+	183.00
RP177	+	189.08
RP178	+	192.88
RP179	+	191.36
RP180	+	194.15

Table B.3 (continued)

RP181	+	190.85
RP182	+	190.35
RP183	+	189.08
RP184	+	194.40
RP185	+	195.67
RP186	+	196.43
RP187	+	196.68

Table B. 4 Data of limit of detection determination study

Sample Number	Artus Quantitative Analysis $\log_{10}$ concentration (copy/ml)	Prototype Fluorescence Intensity	Prototype Qualitative Analysis (+/-)
AQS7-D1-R1	2.35	34.8	+
AQS7-D1-R2	2.35	32.9	+
AQS7-D1-R3	2.35	34.92	+
AQS7-D1-R4	2.35	33.22	+
AQS7-D1-R5	2.35	35.04	+
AQS7-D1-R6	2.35	35.16	+
AQS7-D1-R7	2.35	33.55	+
AQS7-D1-R8	2.35	33.88	+
AQS7-D1-R9	2.35	35.28	+
AQS7-D1-R10	2.35	34.05	+
AQS7-D1-R11	2.35	35.4	+
AQS7-D1-R12	2.35	34.2	+
AQS7-D1-R13	2.35	35.52	+
AQS7-D1-R14	2.35	34.32	+
AQS7-D1-R15	2.35	34.44	+
AQS7-D1-R16	2.35	35.64	+
AQS7-D1-R17	2.35	34.56	+
AQS7-D1-R18	2.35	35.76	+
AQS7-D1-R19	2.35	35.99	+

Table B.4 (continued)

AQS7-D1-R20	2.35	34.68	+
AQS7-D1-R21	2.35	36.33	+
AQS7-D1-R22	2.35	36.83	+
AQS7-D1-R23	2.35	36.67	+
AQS7-D1-R24	2.35	36.8	+
AQS7-D2-R1	2.25	32.3	+
AQS7-D2-R2	2.25	30.3	+
AQS7-D2-R3	2.25	32.42	+
AQS7-D2-R4	2.25	32.54	+
AQS7-D2-R5	2.25	30.6	+
AQS7-D2-R6	2.25	32.65	+
AQS7-D2-R7	2.25	31.05	+
AQS7-D2-R8	2.25	32.76	+
AQS7-D2-R9	2.25	31.38	+
AQS7-D2-R10	2.25	32.87	+
AQS7-D2-R11	2.25	31.5	+
AQS7-D2-R12	2.25	32.99	+
AQS7-D2-R13	2.25	31.62	+
AQS7-D2-R14	2.25	33.12	+
AQS7-D2-R15	2.25	31.74	+
AQS7-D2-R16	2.25	33.24	+
AQS7-D2-R17	2.25	31.86	+
AQS7-D2-R18	2.25	33.36	+
AQS7-D2-R19	2.25	31.98	+
AQS7-D2-R20	2.25	33.69	+
AQS7-D2-R21	2.25	32.05	+
AQS7-D2-R22	2.25	33.99	+
AQS7-D2-R23	2.25	34.3	+
AQS7-D2-R24	2.25	32.18	+
AQS7-D3-R1	2.15	28.25	+
AQS7-D3-R2	2.15	27.99	+
AQS7-D3-R3	2.15	28.52	+
AQS7-D3-R4	2.15	28.82	+
AQS7-D3-R5	2.15	29.72	+
AQS7-D3-R6	2.15	28.91	+
AQS7-D3-R7	2.15	29.81	+

Table B.4 (continued)

AQS7-D3-R8	2.15	29.01	+
AQS7-D3-R9	2.15	29.95	+
AQS7-D3-R10	2.15	29.12	+
AQS7-D3-R11	2.15	30.05	+
AQS7-D3-R12	2.15	29.23	+
AQS7-D3-R13	2.15	30.12	+
AQS7-D3-R14	2.15	29.32	+
AQS7-D3-R15	2.15	30.21	+
AQS7-D3-R16	2.15	29.41	+
AQS7-D3-R17	2.15	30.45	+
AQS7-D3-R18	2.15	29.45	+
AQS7-D3-R19	2.15	30.71	+
AQS7-D3-R20	2.15	29.51	+
AQS7-D3-R21	2.15	30.91	+
AQS7-D3-R22	2.15	29.52	+
AQS7-D3-R23	2.15	31.11	+
AQS7-D3-R24	2.15	29.61	+
AQS7-D4-R1	2.12	29	+
AQS7-D4-R2	2.12	29.06	+
AQS7-D4-R3	2.12	28.01	+
AQS7-D4-R4	2.12	29.12	+
AQS7-D4-R5	2.12	28.15	+
AQS7-D4-R6	2.12	29.18	+
AQS7-D4-R7	2.12	28.3	+
AQS7-D4-R8	2.12	29.24	+
AQS7-D4-R9	2.12	29.3	+
AQS7-D4-R10	2.12	28.46	+
AQS7-D4-R11	2.12	29.36	+
AQS7-D4-R12	2.12	28.52	+
AQS7-D4-R13	2.12	29.42	+
AQS7-D4-R14	2.12	29.48	+
AQS7-D4-R15	2.12	29.65	+
AQS7-D4-R16	2.12	28.58	+
AQS7-D4-R17	2.12	29.82	+
AQS7-D4-R18	2.12	28.64	+
AQS7-D4-R19	2.12	29.99	+

Table B.4 (continued)

AQS7-D4-R20	2.12	28.92	+
AQS7-D4-R21	2.12	28.86	+
AQS7-D4-R22	2.12	28.72	+
AQS7-D4-R23	2.12	28.78	+
AQS7-D4-R24	2.12	28.8	+
AQS7-D5-R1	2.1	28.5	+
AQS7-D5-R2	2.1	27.76	+
AQS7-D5-R3	2.1	28.56	+
AQS7-D5-R4	2.1	27.55	+
AQS7-D5-R5	2.1	28.62	+
AQS7-D5-R6	2.1	27.4	-
AQS7-D5-R7	2.1	28.68	+
AQS7-D5-R8	2.1	28.74	+
AQS7-D5-R9	2.1	27.85	+
AQS7-D5-R10	2.1	28.8	+
AQS7-D5-R11	2.1	28.86	+
AQS7-D5-R12	2.1	28.02	+
AQS7-D5-R13	2.1	28.92	+
AQS7-D5-R14	2.1	28.98	+
AQS7-D5-R15	2.1	29.15	+
AQS7-D5-R16	2.1	28.08	+
AQS7-D5-R17	2.1	29.32	+
AQS7-D5-R18	2.1	28.14	+
AQS7-D5-R19	2.1	29.49	+
AQS7-D5-R20	2.1	28.44	+
AQS7-D5-R21	2.1	28.38	+
AQS7-D5-R22	2.1	28.2	+
AQS7-D5-R23	2.1	28.32	+
AQS7-D5-R24	2.1	28.26	+
AQS7-D6-R1	2.08	27.56	+
AQS7-D6-R2	2.08	27.94	+
AQS7-D6-R3	2.08	28.01	+
AQS7-D6-R4	2.08	28.03	+
AQS7-D6-R5	2.08	26.32	-
AQS7-D6-R6	2.08	28.14	+
AQS7-D6-R7	2.08	27.62	+

Table B.4 (continued)

AQS7-D6-R8	2.08	28.25	+
AQS7-D6-R9	2.08	27.54	+
AQS7-D6-R10	2.08	28.37	+
AQS7-D6-R11	2.08	27.48	+
AQS7-D6-R12	2.08	28.5	+
AQS7-D6-R13	2.08	27.11	-
AQS7-D6-R14	2.08	28.64	+
AQS7-D6-R15	2.08	27.49	+
AQS7-D6-R16	2.08	28.7	+
AQS7-D6-R17	2.08	27.34	-
AQS7-D6-R18	2.08	29.01	+
AQS7-D6-R19	2.08	27.45	+
AQS7-D6-R20	2.08	29.34	+
AQS7-D6-R21	2.08	27.56	+
AQS7-D6-R22	2.08	29.71	+
AQS7-D6-R23	2.08	27.71	+
AQS7-D6-R24	2.08	27.83	+
AQS7-D7-R1	2.05	27.2	-
AQS7-D7-R2	2.05	27.12	-
AQS7-D7-R3	2.05	27.31	-
AQS7-D7-R4	2.05	27.01	-
AQS7-D7-R5	2.05	26.92	-
AQS7-D7-R6	2.05	27.5	+
AQS7-D7-R7	2.05	27.61	+
AQS7-D7-R8	2.05	26.81	-
AQS7-D7-R9	2.05	27.72	+
AQS7-D7-R10	2.05	26.7	-
AQS7-D7-R11	2.05	27.81	+
AQS7-D7-R12	2.05	26.53	-
AQS7-D7-R13	2.05	27.93	+
AQS7-D7-R14	2.05	26.51	-
AQS7-D7-R15	2.05	28	+
AQS7-D7-R16	2.05	26.4	-
AQS7-D7-R17	2.05	28.25	+
AQS7-D7-R18	2.05	26.32	-
AQS7-D7-R19	2.05	28.53	+

Table B.4 (continued)

AQS7-D7-R20	2.05	27.65	+
AQS7-D7-R21	2.05	28.78	+
AQS7-D7-R22	2.05	27.88	+
AQS7-D7-R23	2.05	27.95	+
AQS7-D7-R24	2.05	28.01	+
AQS7-D8-R1	2.02	26.5	-
AQS7-D8-R2	2.02	25.5	-
AQS7-D8-R3	2.02	26.6	-
AQS7-D8-R4	2.02	26.71	-
AQS7-D8-R5	2.02	26.82	-
AQS7-D8-R6	2.02	26.91	-
AQS7-D8-R7	2.02	25.72	-
AQS7-D8-R8	2.02	27.05	-
AQS7-D8-R9	2.02	25.82	-
AQS7-D8-R10	2.02	27.15	-
AQS7-D8-R11	2.02	27.3	-
AQS7-D8-R12	2.02	25.9	-
AQS7-D8-R13	2.02	27.47	+
AQS7-D8-R14	2.02	26	-
AQS7-D8-R15	2.02	27.56	+
AQS7-D8-R16	2.02	26.1	-
AQS7-D8-R17	2.02	27.99	+
AQS7-D8-R18	2.02	28.03	+
AQS7-D8-R19	2.02	26.21	-
AQS7-D8-R20	2.02	28.07	+
AQS7-D8-R21	2.02	26.33	-
AQS7-D8-R22	2.02	27.6	+
AQS7-D8-R23	2.02	27.56	+
AQS7-D8-R24	2.02	26.4	-
AQS7-D9-R1	2	22.54	-
AQS7-D9-R2	2	25.81	-
AQS7-D9-R3	2	22.61	-
AQS7-D9-R4	2	25.99	-
AQS7-D9-R5	2	23.13	-
AQS7-D9-R6	2	26.21	-
AQS7-D9-R7	2	23.73	-

Table B.4 (continued)

AQS7-D9-R8	2	26.43	-
AQS7-D9-R9	2	24.12	-
AQS7-D9-R10	2	26.54	-
AQS7-D9-R11	2	24.34	-
AQS7-D9-R12	2	26.75	-
AQS7-D9-R13	2	24.56	-
AQS7-D9-R14	2	26.96	-
AQS7-D9-R15	2	24.71	-
AQS7-D9-R16	2	27.12	-
AQS7-D9-R17	2	24.94	-
AQS7-D9-R18	2	27.67	+
AQS7-D9-R19	2	25.15	-
AQS7-D9-R20	2	27.64	+
AQS7-D9-R21	2	25.35	-
AQS7-D9-R22	2	27.55	+
AQS7-D9-R23	2	25.4	-
AQS7-D9-R24	2	25.6	-
AQS7-D10-R1	1.95	25.36	-
AQS7-D10-R2	1.95	26.57	-
AQS7-D10-R3	1.95	25.44	-
AQS7-D10-R4	1.95	26.44	-
AQS7-D10-R5	1.95	26.51	-
AQS7-D10-R6	1.95	26.53	-
AQS7-D10-R7	1.95	26.48	-
AQS7-D10-R8	1.95	25.59	-
AQS7-D10-R9	1.95	25.61	-
AQS7-D10-R10	1.95	25.63	-
AQS7-D10-R11	1.95	26.55	-
AQS7-D10-R12	1.95	25.30	-
AQS7-D10-R13	1.95	26.46	-
AQS7-D10-R14	1.95	25.33	-
AQS7-D10-R15	1.95	25.50	-
AQS7-D10-R16	1.95	26.61	-
AQS7-D10-R17	1.95	25.53	-
AQS7-D10-R18	1.95	26.40	-
AQS7-D10-R19	1.95	25.55	-

Table B.4 (continued)

AQS7-D10-R20	1.95	25.46	-
AQS7-D10-R21	1.95	26.59	-
AQS7-D10-R22	1.95	25.48	-
AQS7-D10-R23	1.95	26.42	-
AQS7-D10-R24	1.95	26.32	-
AQS7-D11-R1	1.85	26.64	-
AQS7-D11-R2	1.85	26.34	-
AQS7-D11-R3	1.85	25.36	-
AQS7-D11-R4	1.85	26.36	-
AQS7-D11-R5	1.85	25.38	-
AQS7-D11-R6	1.85	26.66	-
AQS7-D11-R7	1.85	25.40	-
AQS7-D11-R8	1.85	26.30	-
AQS7-D11-R9	1.85	26.68	-
AQS7-D11-R10	1.85	26.62	-
AQS7-D11-R11	1.85	25.32	-
AQS7-D11-R12	1.85	26.38	-
AQS7-D11-R13	1.85	25.34	-
AQS7-D11-R14	1.85	27.12	-
AQS7-D11-R15	1.85	26.72	-
AQS7-D11-R16	1.85	26.24	-
AQS7-D11-R17	1.85	26.03	-
AQS7-D11-R18	1.85	25.42	-
AQS7-D11-R19	1.85	26.28	-
AQS7-D11-R20	1.85	24.67	-
AQS7-D11-R21	1.85	26.70	-
AQS7-D11-R22	1.85	26.04	-
AQS7-D11-R23	1.85	25.26	-
AQS7-D11-R24	1.85	26.82	-
AQS7-D12-R1	1.75	25.99	-
AQS7-D12-R2	1.75	26.01	-
AQS7-D12-R3	1.75	26.26	-
AQS7-D12-R4	1.75	26.02	-
AQS7-D12-R5	1.75	25.39	-
AQS7-D12-R6	1.75	25.42	-
AQS7-D12-R7	1.75	26.78	-

AQS7-D12-R8	1.75	25.45	-
AQS7-D12-R9	1.75	26.74	-
AQS7-D12-R10	1.75	25.28	-
AQS7-D12-R11	1.75	25.96	-
AQS7-D12-R12	1.75	26.90	-
AQS7-D12-R13	1.75	25.94	-
AQS7-D12-R14	1.75	26.00	-
AQS7-D12-R15	1.75	25.98	-
AQS7-D12-R16	1.75	26.22	-
AQS7-D12-R17	1.75	25.97	-
AQS7-D12-R18	1.75	26.21	-
AQS7-D12-R19	1.75	26.10	-
AQS7-D12-R20	1.75	26.93	-
AQS7-D12-R21	1.75	25.63	-
AQS7-D12-R22	1.75	26.05	-
AQS7-D12-R23	1.75	26.86	-
AQS7-D12-R24	1.75	25.30	-

Table B. 5 Data of Figure 4.21

Sample Number	Artus Quantitative Analysis $\log_{10}$ concentration (copy/ml)	Prototype Fluorescence Intensity
AQS1-R1	8.75	186.34
AQS1-R2	8.75	200.98
AQS1-R3	8.75	191.45
AQS1-R4	8.75	197.58
AQS1-R5	8.75	192.67
AQS1-R6	8.75	195.34
AQS1-R7	8.75	193.97
AQS1-R8	8.75	196.35

Table B.5 (continued)

AQS2-R1	7.75	180.41
AQS2-R2	7.75	171.32
AQS2-R3	7.75	179.37
AQS2-R4	7.75	174.36
AQS2-R5	7.75	178.63
AQS2-R6	7.75	175.87
AQS2-R7	7.75	183.92
AQS2-R8	7.75	177.93
AQS3-R1	6.75	138.34
AQS3-R2	6.75	148.82
AQS3-R3	6.75	140.98
AQS3-R4	6.75	145.96
AQS3-R5	6.75	141.87
AQS3-R6	6.75	144.86
AQS3-R7	6.75	142.95
AQS3-R8	6.75	143.87
AQS4-R1	5.75	123.12
AQS4-R2	5.75	116.34
AQS4-R3	5.75	122.32
AQS4-R4	5.75	117.65
AQS4-R5	5.75	121.21
AQS4-R6	5.75	118.73
AQS4-R7	5.75	120.34
AQS4-R8	5.75	119.35
AQS5-R1	4.75	103.12
AQS5-R2	4.75	96.34
AQS5-R3	4.75	101.34
AQS5-R4	4.75	97.36
AQS5-R5	4.75	98.73
AQS5-R6	4.75	99.46
AQS5-R7	4.75	102.45
AQS5-R8	4.75	100.23
AQS6-R1	3.75	65.47
AQS6-R2	3.75	68.99
AQS6-R3	3.75	66.93
AQS6-R4	3.75	66.76

Table B.5 (continued)

AQS6-R5	3.75	67.38
AQS6-R6	3.75	68.63
AQS6-R7	3.75	66.37
AQS6-R8	3.75	67.47
AQS7-R1	2.75	45.34
AQS7-R2	2.75	45.99
AQS7-R3	2.75	45.34
AQS7-R4	2.75	45.79
AQS7-R5	2.75	45.42
AQS7-R6	2.75	45.71
AQS7-R7	2.75	45.5
AQS7-R8	2.75	45.6

Table B. 6 Data of precision study

Sample Number	Artus Quantitative Analysis $\log_{10}$ concentration (copy/ml)	Prototype Fluorescence Intensity	Prototype Quantitative Analysis $\log_{10}$ concentration (copy/ml)
AQS5-intra01	4.75	89.69	4.51
AQS5-intra02	4.75	101.87	4.99
AQS5-intra03	4.75	92.76	4.63
AQS5-intra04	4.75	98.12	4.84
AQS5-intra05	4.75	94.45	4.70
AQS5-intra06	4.75	96.45	4.78
AQS5-intra07	4.75	94.67	4.71
AQS5-intra08	4.75	95.23	4.73
AQS5-inter01	4.75	101.23	4.96
AQS5-inter02	4.75	89.35	4.50
AQS5-inter03	4.75	98.54	4.86
AQS5-inter04	4.75	92.89	4.64
AQS5-inter05	4.75	96.23	4.77
AQS5-inter06	4.75	94.29	4.69

Table B.6 (continued)

AQS5-inter07	4.75	95.23	4.73
AQS5-inter08	4.75	94.67	4.71
AQS5-batch01	4.75	95.29	4.73
AQS5-batch02	4.75	95.23	4.73
AQS5-batch03	4.75	96.87	4.79
AQS5-batch04	4.75	94.56	4.70
AQS5-batch05	4.75	98.38	4.85
AQS5-batch06	4.75	92.76	4.63
AQS5-batch07	4.75	101.99	4.99
AQS5-batch08	4.75	89.01	4.48
AQS5-brand01	4.75	89.7	4.51
AQS5-brand02	4.75	95.42	4.74
AQS5-brand03	4.75	101.11	4.96
AQS5-brand04	4.75	92.12	4.61
AQS5-brand05	4.75	98.71	4.87
AQS5-brand06	4.75	95.42	4.74
AQS5-brand07	4.75	93.64	4.67
AQS5-brand08	4.75	97.2	4.81

Table B. 7 Data of robustness study

Sample Number	Artus Quantitative Analysis $\log_{10}$ concentration (copy/ml)	Prototype Fluorescence Intensity	Prototype Quantitative Analysis $\log_{10}$ concentration (copy/ml)
S-RN001	2.6	38.45	2.49
S-RN002	2.6	39.85	2.55
S-RN003	2.6	41.98	2.63
S-RN004	2.6	38.67	2.50
S-RN005	2.6	39.86	2.55
S-RN006	2.6	40.99	2.59
S-RN007	2.6	38.87	2.51
S-RN008	2.6	39.87	2.55

Table B.7 (continued)

S-RN009	2.6	40.97	2.59
S-RN010	2.6	38.98	2.51
S-RN011	2.6	39.88	2.55
S-RN012	2.6	39.89	2.55
S-RN013	2.6	39.01	2.51
S-RN014	2.6	39.9	2.55
S-RN015	2.6	39.04	2.52
S-RN016	2.6	39.91	2.55
S-RN017	2.6	39.06	2.52
S-RN018	2.6	40.92	2.59
S-RN019	2.6	40.88	2.59
S-RN020	2.6	39.09	2.52
S-RN021	2.6	39.92	2.55
S-RN022	2.6	40.85	2.59
S-RN023	2.6	39.12	2.52
S-RN024	2.6	39.93	2.55
S-RN025	2.6	40.82	2.59
S-RN026	2.6	39.15	2.52
S-RN027	2.6	39.94	2.55
S-RN028	2.6	40.79	2.58
S-RN029	2.6	39.17	2.52
S-RN030	2.6	39.95	2.55
S-RN031	2.6	40.74	2.58
S-RN032	2.6	39.21	2.52
S-RN033	2.6	39.96	2.55
S-RN034	2.6	39.25	2.52
S-RN035	2.6	39.97	2.55
S-RN036	2.6	39.29	2.52
S-RN037	2.6	39.98	2.55
S-RN038	2.6	39.33	2.53
S-RN039	2.6	40.72	2.58
S-RN040	2.6	39.99	2.55
S-RN041	2.6	39.38	2.53
S-RN042	2.6	40.69	2.58
S-RN043	2.6	40.02	2.55
S-RN044	2.6	39.42	2.53

Table B.7 (continued)

S-RN045	2.6	40.03	2.55
S-RN046	2.6	40.63	2.58
S-RN047	2.6	39.45	2.53
S-RN048	2.6	40.04	2.55
S-RN049	2.6	39.48	2.53
S-RN050	2.6	40.05	2.55
S-RN051	2.6	39.5	2.53
S-RN052	2.6	40.06	2.56
S-RN053	2.6	39.52	2.53
S-RN054	2.6	40.07	2.56
S-RN055	2.6	39.54	2.53
S-RN056	2.6	40.08	2.56
S-RN057	2.6	39.56	2.54
S-RN058	2.6	40.6	2.58
S-RN059	2.6	40.09	2.56
S-RN060	2.6	39.58	2.54
S-RN061	2.6	40.12	2.56
S-RN062	2.6	40.56	2.57
S-RN063	2.6	39.6	2.54
S-RN064	2.6	40.13	2.56
S-RN065	2.6	39.62	2.54
S-RN066	2.6	40.15	2.56
S-RN067	2.6	39.63	2.54
S-RN068	2.6	40.53	2.57
S-RN069	2.6	39.64	2.54
S-RN070	2.6	40.17	2.56
S-RN071	2.6	39.65	2.54
S-RN072	2.6	39.66	2.54
S-RN073	2.6	39.67	2.54
S-RN074	2.6	40.19	2.56
S-RN075	2.6	40.49	2.57
S-RN076	2.6	39.68	2.54
S-RN077	2.6	40.21	2.56
S-RN078	2.6	39.69	2.54
S-RN079	2.6	40.23	2.56
S-RN080	2.6	39.7	2.54

Table B.7 (continued)

S-RN081	2.6	40.25	2.56
S-RN082	2.6	39.72	2.54
S-RN083	2.6	40.27	2.56
S-RN084	2.6	39.73	2.54
S-RN085	2.6	40.29	2.56
S-RN086	2.6	39.74	2.54
S-RN087	2.6	39.75	2.54
S-RN088	2.6	39.77	2.54
S-RN089	2.6	40.31	2.57
S-RN090	2.6	39.78	2.54
S-RN091	2.6	40.33	2.57
S-RN092	2.6	39.79	2.54
S-RN093	2.6	40.47	2.57
S-RN094	2.6	39.8	2.54
S-RN095	2.6	40.45	2.57
S-RN096	2.6	40.35	2.57
S-RN097	2.6	40.43	2.57
S-RN098	2.6	39.81	2.55
S-RN099	2.6	40.37	2.57
S-RN100	2.6	39.82	2.55
S-RN101	2.6	40.39	2.57
S-RN102	2.6	39.83	2.55
S-RN103	2.6	40.41	2.57
S-RN104	2.6	39.84	2.55
S-dH$_2$O	2.6	40.37	2.57

Table B. 8 Data of Figure 4.22

Sample Number	Known Quantitative Diagnosis $\log_{10}$ concentration (copy/ml)	Prototype Fluorescence Intensity	Prototype Quantitative Analysis $\log_{10}$ concentration (copy/ml)
RN001	-	26.51	-
RN002	-	26.53	-
RN003	-	26.48	-
RN004	-	25.59	-
RN005	-	25.61	-
RN006	-	25.63	-
RN007	-	26.55	-
RN008	-	25.30	-
RN009	-	26.46	-
RN010	-	25.33	-
RN011	-	25.36	-
RN012	-	26.57	-
RN013	-	25.44	-
RN014	-	26.44	-
RN015	-	25.46	-
RN016	-	26.59	-
RN017	-	25.48	-
RN018	-	26.42	-
RN019	-	25.50	-
RN020	-	26.61	-
RN021	-	25.53	-
RN022	-	26.40	-
RN023	-	25.55	-
RN024	-	26.62	-
RN025	-	25.32	-
RN026	-	26.38	-
RN027	-	25.34	-
RN028	-	26.64	-
RN029	-	26.34	-
RN030	-	25.36	-

Table B.8 (continued)

RN031	-	26.36	-
RN032	-	25.38	-
RN033	-	26.66	-
RN034	-	26.32	-
RN035	-	25.40	-
RN036	-	26.30	-
RN037	-	26.68	-
RN038	-	25.42	-
RN039	-	26.28	-
RN040	-	24.67	-
RN041	-	26.70	-
RN042	-	26.01	-
RN043	-	26.26	-
RN044	-	26.02	-
RN045	-	27.12	-
RN046	-	26.72	-
RN047	-	26.24	-
RN048	-	26.03	-
RN049	-	26.74	-
RN050	-	25.39	-
RN051	-	25.42	-
RN052	-	26.78	-
RN053	-	25.45	-
RN054	-	25.28	-
RN055	-	26.04	-
RN056	-	25.26	-
RN057	-	26.82	-
RN058	-	25.99	-
RN059	-	25.98	-
RN060	-	26.22	-
RN061	-	25.97	-
RN062	-	26.21	-
RN063	-	26.05	-
RN064	-	26.86	-
RN065	-	25.30	-
RN066	-	25.96	-

RN067	-	26.90	-
RN068	-	25.94	-
RN069	-	26.00	-
RN070	-	26.10	-
RN071	-	26.93	-
RN072	-	25.63	-
RN073	-	26.06	-
RN074	-	24.83	-
RN075	-	26.97	-
RN076	-	26.18	-
RN077	-	25.65	-
RN078	-	25.93	-
RN079	-	25.67	-
RN080	-	26.07	-
RN081	-	25.71	-
RN082	-	25.75	-
RN083	-	27.32	-
RN084	-	25.92	-
RN085	-	25.79	-
RN086	-	26.08	-
RN087	-	25.83	-
RN088	-	26.16	-
RN089	-	25.91	-
RN090	-	25.84	-
RN091	-	26.14	-
RN092	-	25.77	-
RN093	-	25.67	-
RN094	-	26.09	-
RN095	-	25.86	-
RN096	-	25.87	-
RN097	-	25.89	-
RN098	-	26.12	-
RN099	-	25.49	-
RN100	-	25.90	-
RN101	-	25.53	-
RN102	-	25.60	-

Table B.8 (continued)

RN103	-	25.92	-
RN104	-	26.11	-
dH$_2$0	-	25.56	-
RP001	2.01	25.42	-
RP002	2.04	27.45	2.06
RP003	2.09	26.69	-
RP004	2.1	26.18	-
RP005	2.13	25.93	-
RP006	2.14	31.25	2.21
RP007	2.22	33.78	2.31
RP008	2.24	28.72	2.11
RP009	2.29	30.74	2.19
RP010	2.32	31.00	2.20
RP011	2.38	36.57	2.42
RP012	2.4	37.08	2.44
RP013	2.41	36.57	2.42
RP014	2.48	37.33	2.45
RP015	2.52	34.29	2.33
RP016	2.56	37.08	2.44
RP017	2.57	37.33	2.45
RP018	2.61	42.40	2.65
RP019	2.65	41.64	2.62
RP020	2.66	42.14	2.64
RP021	2.72	41.38	2.61
RP022	2.79	45.18	2.76
RP023	2.82	49.74	2.94
RP024	2.89	54.05	3.11
RP025	2.91	46.96	2.83
RP026	2.99	49.24	2.92
RP027	3.04	54.05	3.11
RP028	3.08	52.02	3.03
RP029	3.12	59.12	3.31
RP030	3.17	51.26	3.00
RP031	3.22	57.09	3.23
RP032	3.24	61.90	3.42
RP033	3.28	51.26	3.00

RP034	3.33	57.09	3.23
RP035	3.37	62.41	3.44
RP036	3.4	64.94	3.54
RP037	3.4	56.84	3.22
RP038	3.4	65.20	3.55
RP039	3.44	56.58	3.21
RP040	3.45	66.46	3.60
RP041	3.49	62.41	3.44
RP042	3.5	64.69	3.53
RP043	3.52	61.65	3.41
RP044	3.55	67.48	3.64
RP045	3.58	66.21	3.59
RP046	3.61	66.46	3.60
RP047	3.65	70.26	3.75
RP048	3.67	70.52	3.76
RP049	3.69	70.01	3.74
RP050	3.71	62.41	3.44
RP051	3.78	67.48	3.64
RP052	3.78	70.01	3.74
RP053	3.82	76.09	3.97
RP054	3.95	72.80	3.84
RP055	4.02	79.39	4.10
RP056	4.09	76.85	4.00
RP057	4.12	76.60	3.99
RP058	4.18	77.61	4.03
RP059	4.22	84.45	4.30
RP060	4.24	84.45	4.30
RP061	4.27	79.39	4.10
RP062	4.34	83.95	4.28
RP063	4.35	84.71	4.31
RP064	4.4	82.17	4.21
RP065	4.4	84.45	4.30
RP066	4.49	86.48	4.38
RP067	4.5	91.55	4.58
RP068	4.5	92.81	4.63
RP069	4.5	95.60	4.74

Table B.8 (continued)

RP070	4.51	89.77	4.51
RP071	4.56	89.77	4.51
RP072	4.66	91.55	4.58
RP073	4.67	95.60	4.74
RP074	4.67	94.59	4.70
RP075	4.69	89.77	4.51
RP076	4.71	92.05	4.60
RP077	4.78	95.60	4.74
RP078	4.82	96.61	4.78
RP079	4.87	93.32	4.65
RP080	4.94	98.39	4.85
RP081	4.98	96.61	4.78
RP082	5.02	104.21	5.08
RP083	5.1	102.19	5.00
RP084	5.13	104.72	5.10
RP085	5.19	106.75	5.18
RP086	5.23	104.72	5.10
RP087	5.24	107.00	5.19
RP088	5.29	110.04	5.31
RP089	5.34	112.57	5.41
RP090	5.4	109.79	5.30
RP091	5.4	114.35	5.48
RP092	5.43	113.08	5.43
RP093	5.45	118.15	5.63
RP094	5.46	115.36	5.52
RP095	5.49	114.35	5.48
RP096	5.54	112.57	5.41
RP097	5.6	115.36	5.52
RP098	5.6	119.41	5.68
RP099	5.62	119.92	5.70
RP100	5.66	115.36	5.52
RP101	5.67	118.40	5.64
RP102	5.7	119.41	5.68
RP103	5.72	109.79	5.30
RP104	5.79	118.15	5.63
RP105	5.8	120.93	5.74

RP106	5.83	119.41	5.68
RP107	5.91	123.97	5.86
RP108	5.99	126.25	5.95
RP109	6	129.55	6.08
RP110	6	127.52	6.00
RP111	6.03	130.05	6.10
RP112	6.1	132.33	6.19
RP113	6.12	132.84	6.21
RP114	6.13	129.80	6.09
RP115	6.19	132.33	6.19
RP116	6.23	129.80	6.09
RP117	6.28	135.12	6.30
RP118	6.32	137.65	6.40
RP119	6.34	135.12	6.30
RP120	6.45	137.65	6.40
RP121	6.5	142.21	6.58
RP122	6.6	144.75	6.68
RP123	6.6	141.20	6.54
RP124	6.62	146.77	6.76
RP125	6.67	146.27	6.74
RP126	6.7	145.76	6.72
RP127	6.7	141.20	6.54
RP128	6.78	147.03	6.77
RP129	6.8	149.81	6.88
RP130	6.8	151.33	6.94
RP131	6.81	146.77	6.76
RP132	6.89	146.77	6.76
RP133	6.89	150.83	6.92
RP134	6.9	149.81	6.88
RP135	6.9	150.32	6.90
RP136	6.92	148.80	6.84
RP137	7.01	152.09	6.97
RP138	7.03	154.88	7.08
RP139	7.12	158.17	7.21
RP140	7.2	160.45	7.30
RP141	7.22	155.39	7.10

Table B.8 (continued)

RP142	7.23	157.92	7.20
RP143	7.24	159.95	7.28
RP144	7.25	162.48	7.38
RP145	7.29	158.17	7.21
RP146	7.32	160.45	7.30
RP147	7.34	157.92	7.20
RP148	7.35	163.75	7.43
RP149	7.36	161.21	7.33
RP150	7.43	163.24	7.41
RP151	7.49	162.48	7.38
RP152	7.5	166.03	7.52
RP153	7.54	165.77	7.51
RP154	7.54	163.49	7.42
RP155	7.55	166.53	7.54
RP156	7.64	170.08	7.68
RP157	7.65	172.11	7.76
RP158	7.66	170.08	7.68
RP159	7.71	170.59	7.70
RP160	7.72	169.32	7.65
RP161	7.8	170.08	7.68
RP162	7.84	169.32	7.65
RP163	7.89	175.65	7.90
RP164	7.9	175.15	7.88
RP165	7.93	177.17	7.96
RP166	7.97	177.43	7.97
RP167	8.01	177.43	7.97
RP168	8.04	180.72	8.10
RP169	8.1	182.75	8.18
RP170	8.12	183.51	8.21
RP171	8.21	180.72	8.10
RP172	8.22	183.51	8.21
RP173	8.25	184.27	8.24
RP174	8.32	186.55	8.33
RP175	8.34	186.04	8.31
RP176	8.4	183.00	8.19
RP177	8.43	189.08	8.43

Table B.8 (continued)

RP178	8.46	192.88	8.58
RP179	8.47	191.36	8.52
RP180	8.51	194.15	8.63
RP181	8.53	190.85	8.50
RP182	8.54	190.35	8.48
RP183	8.65	189.08	8.43
RP184	8.66	194.40	8.64
RP185	8.7	195.67	8.69
RP186	8.73	196.43	8.72
RP187	8.74	196.68	8.73

<center>**CURRICULUM VITAE**</center>

PERSONEL INFORMATION

Surname, Name: Balcı, Oğuz

Nationality: Turkish (TC)

Date and Place of Birth: 24 October 1979, Sakarya

Marital Status: Married

Phone: +90 530 834 3560

email: oguzbalci@denovo.com.tr

EDUCATION

Degree	Institution	Year of Graduation
MS	METU Biotechnology	2008
BS	METU Food Engineering	2003
High School	Kocaeli Anatolian High School	1997

WORK EXPERIENCE

Year	Place	Enrollment
2009- Present	Denovo Biotechnology Inc.	Founder/R&D Manager
2005-2009	Gazi Unv. Nanomed. Res. Cen.	R&D Engineer
2003-2005	Interlab Inc.	Sales Engineer

PUBLICATIONS

1. Pınar Çalık, Oğuz Balcı, Tunçer H. Özdamar, 2010. Human growth hormone-specific aptamer identification using improved oligonucleotide ligand evolution method. Protein Expression and Purification, Volume 69, Issue 1, January 2010, Pages 21-28.

2. Sevket Tolga Camli, Fatih Buyukserin, Oguz Balci, Gurer Guven Budak, 2010. Size controlled synthesis of sub-100 nm monodisperse poly(methylmethacrylate) nanoparticles using surfactant-free emulsion polymerization. Journal of Colloid and Interface Science 344 (2010) 528–532.

HOBBIES

1. Billiards
2. Guitar